

Redshift distances in flat Friedmann-Lemaître-Robertson-Walker spacetime

Steffen Haase^{*1}

^{*}Leipzig, Germany

Abstract

In the present paper we use the flat Friedmann-Lemaître-Robertson-Walker metric describing a spatially homogeneous and isotropic universe to derive the cosmological redshift distance in a way which differs from that which can be found in the general astrophysical literature.

Using the Friedmann-Lemaître-Robertson-Walker the radial physical distance is described by $R(t) = a(t)r$. In this equation the radial co-moving coordinate is named r and the time-depending scale parameter is named $a(t)$. We use the co-moving coordinate r_e (the subscript e indicates emission) describing the place of a galaxy which is emitting photons and r_a (the subscript a indicates absorption) describing the place of an observer within a different galaxy on which the photons - which were traveling thru the universe - are absorbed. Therefore the physical distance - the real way of light - is calculated by $D = a(t_0)r_a - a(t_e)r_e \equiv R_{0a} - R_{ee}$. Here means $a(t_0)$ the today's (t_0) scale parameter and $a(t_e)$ the scale parameter at the time t_e of emission of the photons. The physical distance D is therefore a difference of two different physical distances from a coordinate origin being on $r = 0$.

Nobody can doubt this real travel way of light: The photons are emitted on the co-moving coordinate place r_e and are than traveling to the co-moving coordinate place r_a . During this traveling the time is moving from t_e to t_0 ($t_e \leq t_0$) and therefore the scale parameter is changing in the meantime from $a(t_e)$ to $a(t_0)$.

Using this right physical distance we calculate the redshift distance and some relevant classical cosmological equations (effects) and compare these theoretical results with some measurements of astrophysics (quasars, SN Ia and black hole).

We get the today's Hubble parameter $H_{0a} \approx 65.66$ km/(s Mpc) as a main result. This value is a little bit smaller than the Hubble parameter $H_{0,Planck} \approx 67.66$ km/(s Mpc) resulting from Planck 2018 data which is discussed in the specialist literature. Furthermore, we find for the radius of the so-called Friedmann sphere $R_{0a} \approx 3,096.92$ Mpc. This radius corresponds to the maximum possible distance of seeing within an expanding universe. Photons, which were emitted at this distance, are infinite red shifted.

The today's mass density of the Friedmann sphere results in $\rho_{0m} \approx 7.82 \times 10^{-29}$ g/cm³. For the mass of the Friedmann sphere we get $M_{Fs} \approx 2.86 \times 10^{56}$ g.

The mass of black hole within the galaxy M87 has the value $M_{BH, M87} \approx 2.36 \times 10^{45}$ g. The redshift distance of this object is $D \approx 19.45$ Mpc but its today's distance is only $D_0 \approx 6.27$ Mpc.

Key words: relativistic astrophysics, theoretical and observational cosmology, redshift, Hubble parameter, quasar, galaxy, M87, SN Ia, black hole

PACS NO:

¹ steffen_haase@vodafone.de

Contents:

1. Introduction	3
1.1 Simplifying assumptions	3
2 Derivation of cosmological relevant relations	4
2.1 Previews	4
2.2 The redshift distance	6
2.3 Hubble parameter	14
2.4 The magnitude-redshift relation	15
2.5 The angular size-redshift relation	16
2.6 The number-redshift relation	17
3. Derivation of further physical redshift distances	19
4. Determination of the parameter values	23
4.1 Magnitude-redshift relation	24
4.2 Number-redshift relation	26
4.3 Angular size-redshift relation	27
4.4 Fixing of R_{0a} with the help of SN Ia	29
4.5 Calculation of the further redshift distances for the SN Ia and M87	31
4.6 Evaluation of the data from the black hole in M87	34
4.7 Maximum values known today: Galaxy UDFj-39546284 and Quasar J0313	36
5 Additions	37
5.1 About the mass of Friedmann sphere	37
5.2 About the derivation of the redshift distance in the specialist literature	39
6. Final considerations	41
6.1 Hubble parameter	42
6.2 Mean values	45
7. Concluding remarks	46
8. Appendix	47

1. Introduction

The current cosmological standard model assumes the correctness of Einstein's field equations (EFE) containing the cosmological term Λ

$$G_{\mu\nu} = \frac{8\pi G}{c_0^4} T_{\mu\nu} - \Lambda g_{\mu\nu} \quad (1)$$

and solves these equations with the help of the Friedmann-Lemaitre-Robertson-Walker metric (FLRWM)

$$ds^2 = c_0^2 dt^2 - a^2(t) \left[\frac{dr^2}{1 - \varepsilon r^2} + r^2 (d\vartheta^2 + \sin^2 \vartheta d\varphi^2) \right], \quad (2)$$

which is suitable for the description of a homogeneous and isotropic universe evolving over time.

The solutions found by solving the EFE are the two Friedmann equations (FE)

$$\left(\frac{\dot{a}}{a} \right)^2 = \frac{8\pi G}{3} \rho - \frac{\varepsilon c_0^2}{a^2} + \frac{\Lambda c_0^2}{3} \quad \text{and} \quad \frac{\ddot{a}}{a} = -\frac{4\pi G}{3} \left(\rho + \frac{3P}{c_0^2} \right) + \frac{\Lambda c_0^2}{3} \quad (3)$$

with $\rho = \sum_i \rho_i \quad i = r, m$.

$G_{\mu\nu}$ is the Einstein tensor, G the gravitational constant, c_0 the light velocity in vacuum, $T_{\mu\nu}$ the energy-momentum tensor and $g_{\mu\nu}$ the metric tensor. The parameter Λ is the cosmological constant that Einstein added to his original field equations, but later discarded. With $\varepsilon = 0, +1$ or -1 the constant of curvature was introduced and r, ϑ and φ are spherical polar coordinates. The time-dependent cosmological scale parameter was designated with $a(t)$ and its time derivatives with points above. P is the pressure of matter and ρ is mainly the sum of two different densities: relativistic radiation (index r) and not-relativistic matter (index m).

1.1 Simplifying assumptions

The application of the theoretical standard cosmology to the measured data of the observational cosmology shows that the universe is very probable flat. For this reason, the curvature constant ε is negligible. We agree with this finding, whereby the FLRWM and the first FE simplify to

$$ds^2 = c_0^2 dt^2 - a^2(t) \left[dr^2 + r^2 (d\vartheta^2 + \sin^2 \vartheta d\varphi^2) \right] \quad (2a)$$

and

$$\frac{\dot{a}^2}{c_0^2} = \frac{K_r}{a^2} + \frac{K_m}{a} + a^2 \frac{\Lambda}{3} \quad (3a)$$

respectively.

Here we have introduced the two conservation laws

$$K_r = \frac{8\pi G}{3c_0^2} (\rho_r a^4) = \text{const} \quad \text{or} \quad \rho_r = \frac{3c_0^2 K_r}{8\pi G} \frac{1}{a^4} \quad (4)$$

and

$$K_m = \frac{8\pi G}{3c_0^2} (\rho_m a^3) = \text{const} \quad \text{or} \quad \rho_m = \frac{3c_0^2 K_m}{8\pi G} \frac{1}{a^3} \quad (5)$$

Eq. (4) describes the development in time of radiation density and Eq. (5) means the equivalent for non-relativistic matter.

In the following, we also neglect the mathematical possible cosmological constant Λ . The comparison of the redshift distance derived within this paper with measurement results shows in retrospect that this additional parameter is not required. As a result, the EFE are returned to their historically original form and the FE takes on the simpler form

$$\frac{\dot{a}^2}{c_0^2} = \frac{K_r}{a^2} + \frac{K_m}{a} \quad (3b)$$

2 Derivation of cosmological relevant relations

2.1 Previews

From the requirement of homogeneity it follows that all extra-galactic objects remain at their co-moving coordinate location r in the course of the temporal development of the universe, i.e. the coordinate distance between randomly selected galaxies does not change over time, the galaxies rest in this co-moving coordinate system. For this reason, $dr/dt = 0$ applies to them.

This does not apply to the freely moving photons in the universe: They detach themselves from a galaxy at a certain point in time at a certain coordinate location, and are then later absorbed at a completely different coordinate location.

Here we introduce the designation r_e (the subscript **e** indicates **e**mission of light) for the coordinate location of the light-emitting galaxy and name the coordinate location of the galaxy in which the observer resides r_a (the subscript **a** indicates **a**bsorption of light). In the Euclidean space ($\varepsilon = 0$) considered here, both variables mark the coordinate distance from the coordinate origin $r = 0$. The constant coordinate distance between the two galaxies is therefore calculated to be $r_a - r_e$ if we assume that the galaxy of the observer is more depart from the coordinate origin as the light-emitting galaxy. The light should therefore move from the inside to the outside within a spherical assumed mass distribution (outgoing photons), which serves as a simple model for the universe (using the FLRWM, it is quite easy to arrange that all directions are of a radial kind).

Due to the measurable expansion of the universe we know that in the course of cosmic evolution all physical distances $R(t) = a(t)r$ over the time-dependent scale parameter $a(t)$ being stretched according to the solution of FE (3b).

For a galaxy resting in the coordinate system of the FLRWM, the real physical distance from the coordinate origin becomes calculated to

$$R(t) = a(t) \int_0^r \frac{d\bar{r}}{\sqrt{1 - \varepsilon \bar{r}^2}} = a(t) r \quad , \quad (6)$$

if $\varepsilon = 0$ is considered. The radial co-moving coordinate r does not depend on time for galaxies.

The physical distance of the light-emitting galaxy from the coordinate origin at time t_e (the time at that time) is therefore

$$R_e(t_e) = a(t_e) r_e \equiv a_e r_e = R_{ee} \quad , \quad (7)$$

while for the analog distance of the galaxy containing the observer at the same time

$$R_a(t_e) = a(t_e) r_a \equiv a_e r_a = R_{ea} \quad (8)$$

applies. The physical distance of both galaxies at the time t_e is therefore

$$D(t_e) = D_e = a_e r_a - a_e r_e = a_e (r_a - r_e) = R_{ea} - R_{ee} \quad . \quad (9)$$

For the distance between both cosmic objects at a later time - means today's time - $t_0 > t_e$ then applies

$$D(t_0) = D_0 = a_0 r_a - a_0 r_e = a_0 (r_a - r_e) = R_{0a} - R_{0e} \quad . \quad (10)$$

However, both distances mentioned above are worthless for the computation of cosmological relevant relations, since the emitted photons make their way to the observer, which has to be calculated in accordance with

$$D = a_0 r_a - a_e r_e = R_{0a} - R_{ee} \quad . \quad (11)$$

To see this, imagine a photon that detaches itself at the time $t_e < t_0$ from the emitting galaxy at the coordinate r_e , where the scale parameter at this time has the value a_e . After the photon has moved freely through the universe, it will arrive at the coordinate point r_a , the place of the observer within another galaxy, at time t_0 , with the scale parameter at that time being a_0 . Thus, the photon does not travel the path described by Eq. (9) nor by Eq. (10). The real distance traveled by the photon is always greater than any one of these distances. This must be taken into account when deriving the redshift distance.

The real physical light path is illustrated by the green line in Fig. 1:

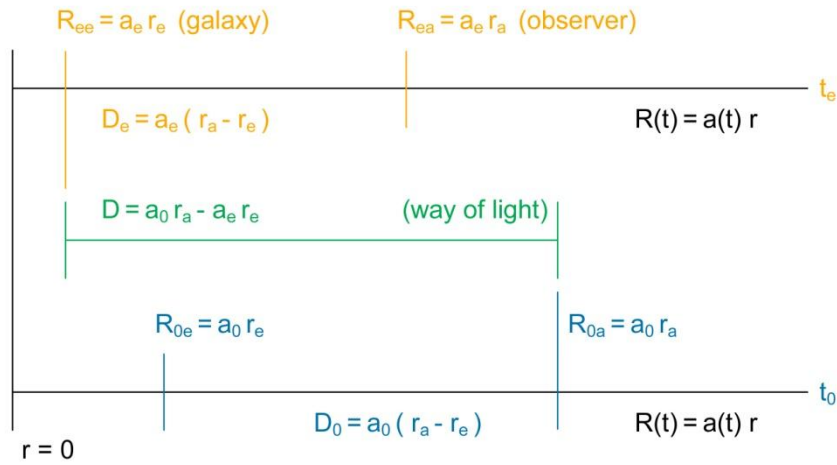


Figure 1. Real physical light path.

These remarks may be sufficient as a preliminary to the now following derivation of the redshift distance.

2.2 The redshift distance

We now want to investigate which equation results for the redshift distance (corresponding to the photon path), which depends on the redshift z , if the integral

$$\int_{r_e}^{r_a} dr = + \int_{t_e}^{t_0} \frac{c_0 dt}{a(t)} \quad (12)$$

is used. This integral results for $\varepsilon = 0$ when the line element ds is set equal to zero in the FLRWM (2a) and radial ($\vartheta = \varphi = \text{const}$) outgoing photons are considered. Eq. (12) describes the motion of photons in the universe traveling from the co-moving coordinate r_e to the co-moving coordinate r_a .

During the travel time of the photons, the scale parameter changes from $a(t_e) = a_e$ to $a(t_0) = a_0$. If the time differential is replaced using the FE (3b), follows from Eq. (12)

$$\int_{r_e}^{r_a} dr = + \int_{a_e}^{a_0} \frac{da}{\sqrt{K_r + a K_m}} \quad . \quad (13)$$

After the execution of the integral we get

$$r_a - r_e = \frac{2}{K_{0m}} \left(\sqrt{K_{0r} + K_{0m} a_0} - \sqrt{K_{er} + K_{em} a_e} \right) \quad . \quad (14)$$

We have used the appropriate terms for both involved conservation laws [see Eq. (16)].

Some further simple calculation steps result in

$$r_a - r_e = \frac{2}{a_0 \sqrt{\frac{8\pi G}{3c_0^2} \rho_{0m}}} \left(\sqrt{1 + \frac{\rho_{0r}}{\rho_{0m}}} - \frac{a_e^2}{a_0^2} \sqrt{\frac{\rho_{er}}{\rho_{0m}}} \sqrt{1 + \frac{\rho_{em}}{\rho_{er}}} \right) \quad (15)$$

because of

$$K_{0m} = \frac{8\pi G}{3c_0^2} \rho_{0m} a_0^3 = \frac{8\pi G}{3c_0^2} \rho_{em} a_e^3 = K_{em} \equiv K_m \quad \text{and} \quad K_{0r} = \frac{8\pi G}{3c_0^2} \rho_{0r} a_0^4 = \frac{8\pi G}{3c_0^2} \rho_{er} a_e^4 = K_{er} \equiv K_r$$

or

$$\frac{K_{0r}}{K_{0m}} = \frac{\rho_{0r}}{\rho_{0m}} a_0 \quad \text{and} \quad \frac{K_{er}}{K_{0m}} = \frac{\rho_{er}}{\rho_{0m}} \frac{a_e^4}{a_0^3} \quad \text{and} \quad \frac{K_{em}}{K_{er}} = \frac{\rho_{em}}{\rho_{er} a_e} \quad . \quad (16)$$

Now we multiply both sides with a_0 and get

$$a_0 r_a - a_0 r_e = \frac{2}{\sqrt{\frac{8\pi G}{3c_0^2} \rho_{0m}}} \left(\sqrt{1 + \frac{\rho_{0r}}{\rho_{0m}}} - \frac{a_e^2}{a_0^2} \sqrt{\frac{\rho_{er}}{\rho_{0m}}} \sqrt{1 + \frac{\rho_{em}}{\rho_{er}}} \right) \quad . \quad (17)$$

On the left side of Eq. (17) is not yet the real path traveled by the photon, but the today's physical distance D_0 of the two galaxies involved.

We now introduce the redshift named z . To this end, we recall the simple relation between the scale parameters at two different times t_e and t_0 and the redshift

$$\frac{a_0}{a_e} = 1 + z \quad \text{or} \quad \frac{a_e^2}{a_0^2} = \frac{1}{(1+z)^2} \quad (18a, b)$$

and also

$$a_0 = (1+z)a_e \quad . \quad (18c)$$

If Eq. (18b) and (18c) are inserted into Eq. (17), the result is

$$a_0 r_a - (1+z)a_e r_e = \frac{2}{\sqrt{\frac{8\pi G}{3c_0^2} \rho_{0m}}} \left(\sqrt{1 + \frac{\rho_{0r}}{\rho_{0m}}} - \frac{1}{(1+z)^2} \sqrt{\frac{\rho_{er}}{\rho_{0m}}} \sqrt{1 + \frac{\rho_{em}}{\rho_{er}}} \right) . \quad (19)$$

Next, all unknown variables have to be eliminated from Eq. (19). Therefore we use the light path D introduced by Eq. (11)

$$a_e r_e = a_0 r_a - D = R_{0a} - D \quad (11a)$$

to find

$$D = \frac{R_{0a}}{(1+z)} \left\{ \frac{2}{R_{0a} \sqrt{\frac{8\pi G}{3c_0^2} \rho_{0m}}} \left[\sqrt{1 + \frac{\rho_{0r}}{\rho_{0m}}} - \frac{1}{(1+z)^2} \sqrt{\frac{\rho_{er}}{\rho_{0m}}} \sqrt{1 + \frac{\rho_{em}}{\rho_{er}}} \right] + z \right\} . \quad (20)$$

Using

$$\begin{aligned} \rho_{0m} a_0^3 &= \rho_{em} a_e^3 & \text{and} & & \rho_{0r} a_0^4 &= \rho_{er} a_e^4 \\ \text{means} & & & & & \\ \rho_{em} &= \rho_{0m} \frac{a_0^3}{a_e^3} & \text{and} & & \rho_{er} &= \rho_{0r} \frac{a_0^4}{a_e^4} & \text{or} & & \frac{1}{\rho_{er}} &= \frac{1}{\rho_{0r}} \frac{a_e^4}{a_0^4} \end{aligned} \quad (21)$$

we find after some simple calculation steps

$$D = \frac{R_{0a}}{(1+z)} \left\{ \frac{2}{R_{0a} \sqrt{\frac{8\pi G}{3c_0^2} \rho_{0m}}} \left[\sqrt{1 + \frac{\rho_{0r}}{\rho_{0m}}} - \frac{1}{(1+z)^2} \frac{a_0^2}{a_e^2} \sqrt{\frac{\rho_{0r}}{\rho_{0m}} + \frac{a_e}{a_0}} \right] + z \right\} . \quad (22)$$

This results in

$$D = \frac{R_{0a}}{(1+z)} \left\{ \frac{2c_0}{R_{0a} \sqrt{\frac{8\pi G}{3} \rho_{0m}}} \left[\sqrt{1 + \frac{\rho_{0r}}{\rho_{0m}}} - \sqrt{\frac{\rho_{0r}}{\rho_{0m}} + \frac{1}{(1+z)}} \right] + z \right\} . \quad (23)$$

As further abbreviations we introduce now

$$\frac{1}{\beta_{0m}} = \frac{2c_0}{R_{0a} \sqrt{\frac{8\pi G \rho_{0m}}{3}}} = \frac{c_0}{V_0} \quad \text{and} \quad \Omega_{0rm} = \frac{\rho_{0r}}{\rho_{0m}} \quad (24a,b)$$

and get therefore

$$D(z; R_{0a}, \beta_{0m}, \Omega_{0rm}) = \frac{R_{0a}}{(1+z)} \left\{ \frac{1}{\beta_{0m}} \left[\sqrt{1 + \Omega_{0rm}} - \sqrt{\Omega_{0rm} + \frac{1}{(1+z)}} \right] + z \right\} . \quad (25)$$

This is the equation for the redshift distance, for which we were searching.

The parameter Ω_{0rm} denotes the today's ratio of radiation density and non-relativistic matter density how it is used in the specialist literature.

The redshift distance D is therefore a function of z and the three parameters R_{0a} , β_{0m} and Ω_{0rm} which all can be determined fundamental by fitting the equation to appropriate astrophysical measurements.

The name β_{0m} was chosen for the second parameter because it is a today's quotient of two velocities, where the denominator is the speed of light in vacuum named c_0 .

The astrophysical literature does not know the parameter β_{0m} . It results from the non-zeroing of r_a for the observer and of $r_e \neq 0$ for the observed galaxy, respectively.

Now we can have a look at some possibilities of values belonging to the three parameters.

At first we can neglect the parameter Ω_{0rm} if the today's radiation density is very small in comparison of non-relativistic matter density and find in this way

$$D(z; R_{0a}, \beta_{0m}) = \frac{R_{0a}}{(1+z)} \left[\frac{1}{\beta_{0m}} \left(1 - \frac{1}{\sqrt{1+z}} \right) + z \right] . \quad (26)$$

We published this equation already in [11].

For $\Omega_{0rm} \neq 0$ and $\beta_{0m} = 1$ the following equation results

$$D(z; R_{0a}, \Omega_{0rm}) = \frac{R_{0a}}{(1+z)} \left[\sqrt{1 + \Omega_{0rm}} - \sqrt{\Omega_{0rm} + \frac{1}{(1+z)}} + z \right] . \quad (27)$$

If we want additional neglect the today's density of radiation in Eq. (27) we get the simpler equation

$$D(z; R_{0a}) = R_{0a} \left[1 - \frac{1}{(1+z)\sqrt{1+z}} \right] . \quad (28)$$

We now give another expression for $1/\beta_{0m}$:

$$\frac{1}{\beta_{0m}} = \frac{2c_0}{R_{0a} \sqrt{\frac{8\pi G \rho_{0m}}{3}}} = 2 \sqrt{\frac{R_{0a}}{R_S}} . \quad (29)$$

We have used

$$R_S = \frac{2M_{Fs}G}{c_0^2} \quad \text{and} \quad M_{Fs} = \frac{4\pi}{3} \rho_{0m} R_{0a}^3 . \quad (30)$$

With $R_S = 2M_{Fs}G/c_0^2$, the Schwarzschild radius of mass M_{Fs} of the so-called Friedmann sphere was introduced for pure formal reason. It does not play the same role here in cosmology as it does within the Schwarzschild metric.

The mass M_{Fs} takes into consideration all non-relativistic gravitational effective components of the visible universe: $M_{Fs} = \sum M_i$. These can also be different energy components E_i , to which, according to Einstein's energy-mass relationship $M_i = E_i/c^2$, masses M_i can be assigned.

In addition, with M_{Fs} as the total mass, mass components that are invisible to us - perhaps only so far - are taken in to consideration.

Therefore, we can rewrite the redshift distance as

$$D(z; R_{0a}, R_S, \Omega_{0rm}) = \frac{R_{0a}}{(1+z)} \left\{ 2 \sqrt{\frac{R_{0a}}{R_S}} \left[\sqrt{1 + \Omega_{0rm}} - \sqrt{\Omega_{0rm} + \frac{1}{(1+z)}} \right] + z \right\} . \quad (25a)$$

For $\beta_{0m} = 1/2$ we get $R_{0a} = R_S$. In this case, we could believe that every observer is places (formally) on the surface of a black hole (corresponding to the Friedmann sphere) and that he always looks into a black hole while observing.

For a galaxy located in the center of the Friedmann sphere, an observer would measure an infinitely large redshift. Overall, that could be logical.

For $\beta_{0m} = 1$, $R_{0a} = R_S/4$ results and the speed V_0 would be exactly identical to the today's speed of light c_0 .

If the comparison with the measurement data would show $\beta_{0m} = 1$, we would get

$$D(z; R_S, \Omega_{0rm}) = \frac{R_S}{4} \frac{1}{(1+z)} \left[\sqrt{1 + \Omega_{0rm}} - \sqrt{\Omega_{0rm} + \frac{1}{(1+z)}} + z \right] \quad (31)$$

because of then

$$\frac{1}{\beta_{0m}} = 1 = 2 \sqrt{\frac{R_{0a}}{R_S}} \quad or \quad R_{0a} = \frac{R_S}{4} . \quad (29a)$$

In this case, we would immediately see that the total mass M_{Fs} of the Friedmann sphere goes directly into the equation in form of the formally introduced Schwarzschild radius R_S (instead of R_S and R_{0a} at the same time). Therefore, R_S could be used as a scale of cosmological distances.

Fig. 2 shows the redshift distance (25) normalized to the distance R_{0a} for various values of the parameter β_{0m} and $\Omega_{0rm} = 0$.

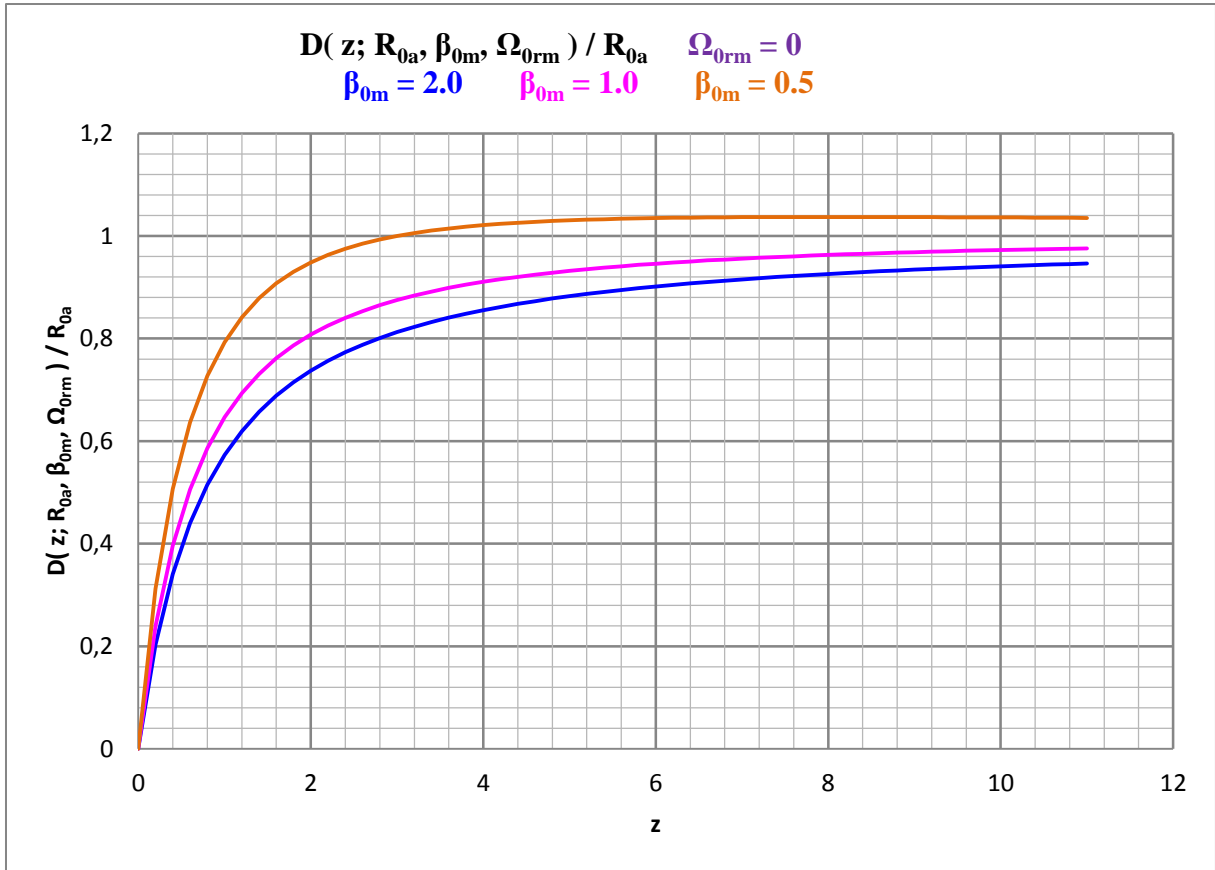


Figure 2. Redshift distance for different values of the parameter β_{0m} and $\Omega_{0rm} = 0$.

Fig. 3 shows the redshift distance (25) normalized to the distance R_{0a} for various values of the parameter Ω_{0rm} and $\beta_{0m} = 1$.

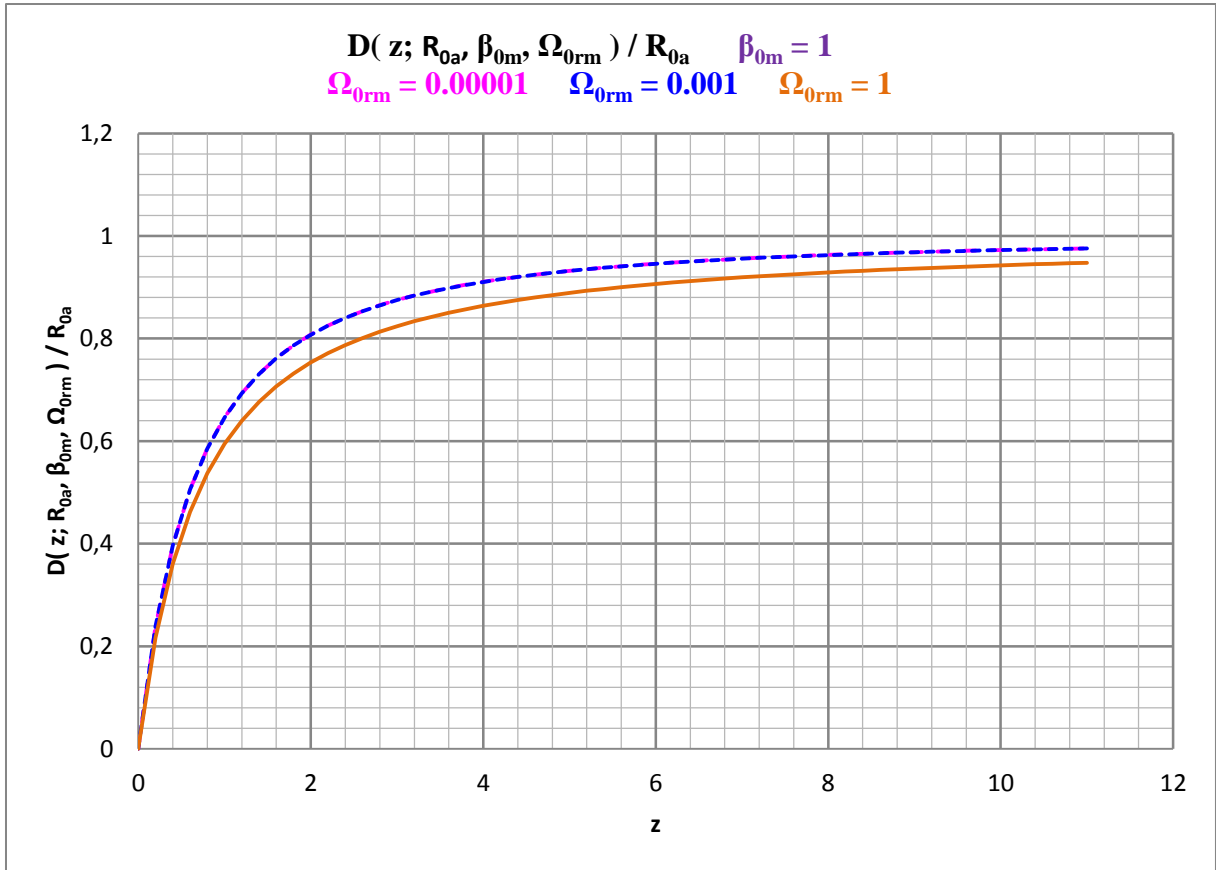


Figure 3. Redshift distance for different values of the parameter Ω_{0rm} and $\beta_{0m} = 1$.

The curvature of the curves is a direct consequence of the Friedmann equation.

For $\beta_{0m} = 1$, the redshift distance $D = R_{0a}$ is achieved for $z = \infty$.

The comparison of Eq. (25) and (25a), respectively, with a Hubble diagram thus determines the current radius $R_{0a} = a_0 r_a$ of the Friedmann sphere (today's physical location of the observer) and its Schwarzschild radius R_S .

Overall, each observer is located on the surface of all imaginable Friedmann spheres around him (for each viewing direction a Friedmann sphere with the radius R_{0a} belongs). The extra-galactic objects (placed on $r = r_e$) observed by him then all lie according to their redshift z on a radial line somewhere between the observer (placed on $r = r_a$) and the center of the Friedmann sphere (placed on $r = 0$).

The physical radius $R_{0a} = a(t_0)r_a$ of the Friedmann sphere changes in reality with time and forms always a limit of visibility, which is growing with time: $R_a(t) = a(t)r_a$.

Outside of every imaginable Friedmann sphere - means here the opposite of observer - there is also mass, which, however, has no gravitational effect to the place of the observer.

It should be mentioned extra that the conceivable Friedmann spheres naturally at least partially overlap.

An increasing limit distance R_{0a} decreases with time the velocity V_0 introduced above, because R_S is a constant. Because Eq. (25) and (25a), respectively, describes the physical behavior of photons in the universe, the velocity V_0 in Eq. (24) could be interpreted as an effective speed of light c_{0*} in vacuum:

$$V_0 = \frac{R_{0a}}{2} \sqrt{\frac{8\pi G \rho_{0m}}{3}} = \frac{c_0}{2} \sqrt{\frac{R_S}{R_{0a}}} \equiv c_{0*} \quad . \quad (24a)$$

This velocity changes according to R_{0a} and ρ_{0m} , respectively, over the time and has for us as today's observers - because of very probable $\beta_{0m} = 1$ - just the value of the vacuum velocity c_0 that we can measure today.

If this interpretation is correct, the effective speed of light c_{0*} was infinitely large at the beginning of the expansion of the universe, because at that time the Friedmann sphere was infinitely small and its matter density was infinitely large, respectively. There is therefore no problem with speeds, which are apparently greater than today's speed of light, when looking into the visible universe

2.3 Hubble parameter

For calculating the Hubble parameter we take a Taylor series expansion of our redshift distance (25) up to first order in z and find

$$D(z; R_{0a}, \beta_{0m}, \Omega_{0rm}) \approx R_{0a} \left(\frac{1}{2\beta_{0m}} \frac{1}{\sqrt{\Omega_{0rm} + 1}} + 1 \right) z + \dots \quad . \quad (32)$$

This results in

$$c_0 z \approx \frac{c_0}{\left(\frac{1}{2\beta_{0m}} \frac{1}{\sqrt{\Omega_{0rm} + 1}} + 1 \right) R_{0a}} D \quad . \quad (33)$$

This is how we find today's Hubble parameter

$$H_{0a}(R_{0a}, \beta_{0m}, \Omega_{0rm}) \approx \frac{c_0}{\left(\frac{1}{2\beta_{0m}} \frac{1}{\sqrt{\Omega_{0rm} + 1}} + 1 \right) R_{0a}} \quad . \quad (34)$$

The Hubble parameter H_{0a} depends on the parameters R_{0a} and Ω_{0rm} and on the speed quotient β_{0m} introduced above and is in this form valid only for small redshifts because of the series expansion made. This means that this H_{0a} is only valid locally.

If $\beta_{0m} = 1$ we find

$$H_{0a}(R_{0a}, \Omega_{0rm}) \approx \frac{c_0}{\left(\frac{1}{2\sqrt{\Omega_{0rm} + 1}} + 1 \right) R_{0a}} \quad . \quad (35)$$

The reciprocal of this Hubble parameter is the Hubble time $t_{H_{0a}}$ in case of $\beta_{0m} = 1$ and setting $\Omega_{0rm} = 0$ yields

$$t_{H_{0a}} = \frac{3R_{0a}}{2c_0} \quad . \quad (36)$$

This simple equation can be found in the specialist literature for flat spaces.

If we consider the today's Hubble parameter (34) obtained above for small redshifts as a definition, we can write the redshift distance via

$$\frac{1}{\beta_{0m}} \approx 2\sqrt{1 + \Omega_{0rm}} \left(\frac{c_0}{H_{0a} R_{0a}} - 1 \right) \quad (34a)$$

also like this

$$D(z; R_{0a}, R_{H_{0a}}, \Omega_{0rm}) = \frac{R_{0a}}{(1+z)} \left\{ 2\sqrt{\Omega_{0rm} + 1} \left(\frac{R_{H_{0a}}}{R_{0a}} - 1 \right) \left[\sqrt{1 + \Omega_{0rm}} - \sqrt{\Omega_{0rm} + \frac{1}{(1+z)}} \right] + z \right\} \quad . \quad (37)$$

The quotient $R_{H_{0a}} = c_0/H_{0a}$ is called the Hubble radius in the astrophysical literature. For this distance, the escape speed by definition reaches the speed of light if it is assumed that a linear Hubble law is valid for all distances, which is - of course - a rough approximation. The Eq. (37) is therefore only valid for small redshifts how the equations (32) and (34) itself.

2.4 The magnitude-redshift relation

The magnitude-redshift relation results by the definition of the apparent magnitude m

$$m - m_{0a} = 5 \log_{10} \frac{D}{R_{0a}} \quad . \quad (38)$$

Here an apparent limit magnitude m_{0a} was introduced for R_{0a} , which also changes with time. Substituting Eq. (25) into Eq. (38) then provides the sought magnitude-redshift relation

$$m(z; m_{0a}, \beta_{0m}, \Omega_{0rm}) = 5 \log_{10} \left\{ \frac{1}{\beta_{0m}} \left[\sqrt{1 + \Omega_{0rm}} - \sqrt{\Omega_{0rm} + \frac{1}{(1+z)}} \right] + z \right\} - 5 \log_{10}(1+z) + m_{0a} \quad . \quad (39)$$

The three free parameters m_{0a} , β_{0m} and Ω_{0rm} can be determined by direct comparison with a magnitude-redshift diagram of astrophysical objects.

For $\beta_{0m} = 1$, the following simpler equation results

$$m(z; m_{0a}, \Omega_{0rm}) = 5 \log_{10} \left[\sqrt{1 + \Omega_{0rm}} - \sqrt{\Omega_{0rm} + \frac{1}{(1+z)}} + z \right] - 5 \log_{10}(1+z) + m_{0a} \quad . \quad (39a)$$

If we ignore in addition the radiation within our equation, we get

$$m(z; m_{0a}) = 5 \log_{10} \left[1 - \frac{1}{(1+z)\sqrt{1+z}} \right] + m_{0a} \quad (39b)$$

We published this equation already in [11].

For comparison, reference is made to Eq. (66) from chapter 5.2, which is known from the specialist literature.

Please be aware that the parameter β_{0m} is not known in the astrophysical literature.

2.5 The angular size-redshift relation

This relation results in for large distances over

$$\varphi = \arcsin \frac{\delta}{D} \approx \frac{\delta}{D} \quad (40)$$

to

$$\varphi(z; \delta / R_{0a}, \beta_{0m}, \Omega_{0rm}) = \frac{\delta}{R_{0a}} \frac{(1+z)}{\left\{ \frac{1}{\beta_{0m}} \left[\sqrt{1+\Omega_{0rm}} - \sqrt{\Omega_{0rm} + \frac{1}{(1+z)}} \right] + z \right\}} \quad (41)$$

In this equation φ means the measurable angular size and δ the linear size of the observed extra-galactic object.

Using $\beta_{0m} = 1$ we get

$$\varphi(z; \delta / R_{0a}, \Omega_{0rm}) = \frac{\delta}{R_{0a}} \frac{(1+z)}{\left[\sqrt{1+\Omega_{0rm}} - \sqrt{\Omega_{0rm} + \frac{1}{(1+z)}} + z \right]} \quad (41a)$$

In logarithmic form Eq. (41) becomes to

$$\log_{10} \varphi(z; \delta / R_{0a}, \beta_{0m}, \Omega_{0rm}) = \log_{10} \frac{\delta}{R_{0a}} - \log_{10} \left\{ \frac{1}{\beta_{0m}} \left[\sqrt{1+\Omega_{0rm}} - \sqrt{\Omega_{0rm} + \frac{1}{(1+z)}} \right] + z \right\} + \log_{10}(1+z) \quad (42)$$

With $\beta_{0m} = 1$ we get the simplified equation

$$\log_{10} \varphi(z; \delta / R_{0a}, \Omega_{0rm}) = \log_{10} \frac{\delta}{R_{0a}} - \log_{10} \left\{ \sqrt{1+\Omega_{0rm}} - \sqrt{\Omega_{0rm} + \frac{1}{(1+z)}} + z \right\} + \log_{10}(1+z) \quad (42a)$$

If we ignore in additional the radiation within our equation, we get

$$\log_{10} \varphi(z; \delta / R_{0a}) = \log_{10} \frac{\delta}{R_{0a}} - \log_{10} \left[1 - \frac{1}{(1+z)\sqrt{1+z}} \right] \quad (42b)$$

We published this equation already in [11].

For comparison, reference is made to Eq. (67) from chapter 5.2, which is known from the specialist literature.

2.6 The number-redshift relation

In flat Euclidean space the equation for the light-path sphere becomes to

$$V = \frac{4\pi}{3} D^3 \quad . \quad (43)$$

If we introduce the redshift distance via Eq. (25)

$$V(z; R_{0a}, \beta_{0m}, \Omega_{0rm}) = \frac{4\pi}{3} \frac{R_{0a}^3}{(1+z)^3} \left\{ \frac{1}{\beta_{0m}} \left[\sqrt{1+\Omega_{0rm}} - \sqrt{\Omega_{0rm} + \frac{1}{(1+z)}} \right] + z \right\}^3 \quad (44)$$

we get for the number-redshift relation

$$N(z; N_{0a}, \beta_{0m}, \Omega_{0rm}) = \frac{N_{0a}}{(1+z)^3} \left\{ \frac{1}{\beta_{0m}} \left[\sqrt{1+\Omega_{0rm}} - \sqrt{\Omega_{0rm} + \frac{1}{(1+z)}} \right] + z \right\}^3 \quad , \quad (45)$$

where N_{0a} means the expected number of objects in the whole light-path sphere V_{0a} and besides

$$N_{0a} = V_{0a} \eta = \frac{4\pi}{3} R_{0a}^3 \eta \quad \text{and} \quad N = V \eta \quad (46a, b)$$

applies. With η the number density was named. In logarithmic form results

$$\log_{10} N(z; N_{0a}, \beta_{0m}, \Omega_{0rm}) = 3 \log_{10} \left\{ \frac{1}{\beta_{0m}} \left[\sqrt{1+\Omega_{0rm}} - \sqrt{\Omega_{0rm} + \frac{1}{(1+z)}} \right] + z \right\} - 3 \log_{10}(1+z) + \log_{10} N_{0a} \quad . \quad (47)$$

If we here also set $\beta_{0m} = 1$, we get

$$\log_{10} N(z; N_{0a}, \Omega_{0rm}) = 3 \log_{10} \left[\sqrt{1+\Omega_{0rm}} - \sqrt{\Omega_{0rm} + \frac{1}{(1+z)}} + z \right] - 3 \log_{10}(1+z) + \log_{10} N_{0a} \quad . \quad (47a)$$

If we ignore in additional the radiation within our equation, we find

$$\log_{10} N(z; N_{0a},) = 3 \log_{10} \left[1 - \frac{1}{(1+z)\sqrt{1+z}} \right] + \log_{10} N_{0a} \quad . \quad (47b)$$

We published this equation already in [11].

For comparison, reference is made to Eq. (68) from chapter 5.2, which is known from the astrophysical literature.

3. Derivation of further physical redshift distances

The starting point for the derivation of the further redshift distances are the following elementary equations

$$(1+z) = \frac{a_0}{a_e} \quad (18a) \quad \text{and} \quad D = R_{0a} - R_{ee} \quad (11)$$

$$\text{and} \quad (1+z) = \frac{a_0 r_a}{a_e r_e} = \frac{R_{0a}}{R_{ea}} \quad \text{and} \quad (1+z) = \frac{a_0 r_e}{a_e r_e} = \frac{R_{0e}}{R_{ee}} \quad (48)$$

and

$$D_e = R_{ea} - R_{ee} = \frac{R_{0a}}{(1+z)} - (R_{0a} - D) = R_{0a} \left[\frac{1}{(1+z)} - 1 \right] + D$$

because of

$$R_{ee} = R_{0a} - D \quad \text{and} \quad R_{ea} = \frac{R_{0a}}{(1+z)} \quad (49)$$

and also

$$D_0 = R_{0a} - R_{0e} = R_{0a} - (1+z)(R_{0a} - D)$$

because of

$$R_{0e} = (1+z)(R_{0a} - D) \quad . \quad (50)$$

This results in the following further distances

$$R_{ee} = R_{0a} - D \quad \text{and} \quad R_{ea} = \frac{R_{0a}}{(1+z)}$$

$$\text{and} \quad R_{0e} = (1+z)R_{ee} = (1+z)(R_{0a} - D) \quad . \quad (51)$$

R_{ee} is the distance at that time between the galaxy emitting the light and the origin of the coordinates at the time t_e the light was emitted (t_e : time at that time).

R_{ea} is the distance at that time of the observer's galaxy from the origin of the coordinates at the time t_e .

R_{0e} is the today's - at time t_0 , at which the light is absorbed by the observer - distance of the light-emitting galaxy from the origin of the coordinates.

R_{0a} is today's distance of the galaxy containing the observer from the origin of the coordinates.

These distances become concretely with Eq. (25)

$$R_{ee}(z; R_{0a}, \beta_{0m}, \Omega_{0rm}) = R_{0a} \left\{ 1 - \frac{1}{(1+z)} \left\{ \frac{1}{\beta_{0m}} \left[\sqrt{1 + \Omega_{0rm}} - \sqrt{\Omega_{0rm} + \frac{1}{(1+z)}} \right] + z \right\} \right\} \quad (52)$$

and

$$R_{0e}(z; R_{0a}, \beta_{0m}, \Omega_{0rm}) = R_{0a} \left\{ 1 - \frac{1}{\beta_{0m}} \left[\sqrt{1 + \Omega_{0rm}} - \sqrt{\Omega_{0rm} + \frac{1}{(1+z)}} \right] \right\} \quad (53)$$

and of course too

$$R_{ea}(z; R_{0a}) = \frac{R_{0a}}{(1+z)} \quad (54)$$

These distances from the coordinate origin yield

$$D_e(z; R_{0a}, \beta_{0m}, \Omega_{0rm}) = R_{0a} \left\{ \frac{1}{(1+z)} \left\{ 1 + \left\{ \frac{1}{\beta_{0m}} \left[\sqrt{1 + \Omega_{0rm}} - \sqrt{\Omega_{0rm} + \frac{1}{(1+z)}} \right] + z \right\} \right\} - 1 \right\} \quad (55)$$

D_e is the distance at that time between the observed galaxy and the galaxy in which the observer is located.

Furthermore we find

$$D_0(z; R_{0a}, \beta_{0m}, \Omega_{0rm}) = \frac{R_{0a}}{\beta_{0m}} \left[\sqrt{1 + \Omega_{0rm}} - \sqrt{\Omega_{0rm} + \frac{1}{(1+z)}} \right] \quad (56)$$

D_0 is the today's distance between the two participating galaxies.

The following figures illustrate the equations for the further redshift distances, where we have normalized all distances to R_{0a} .

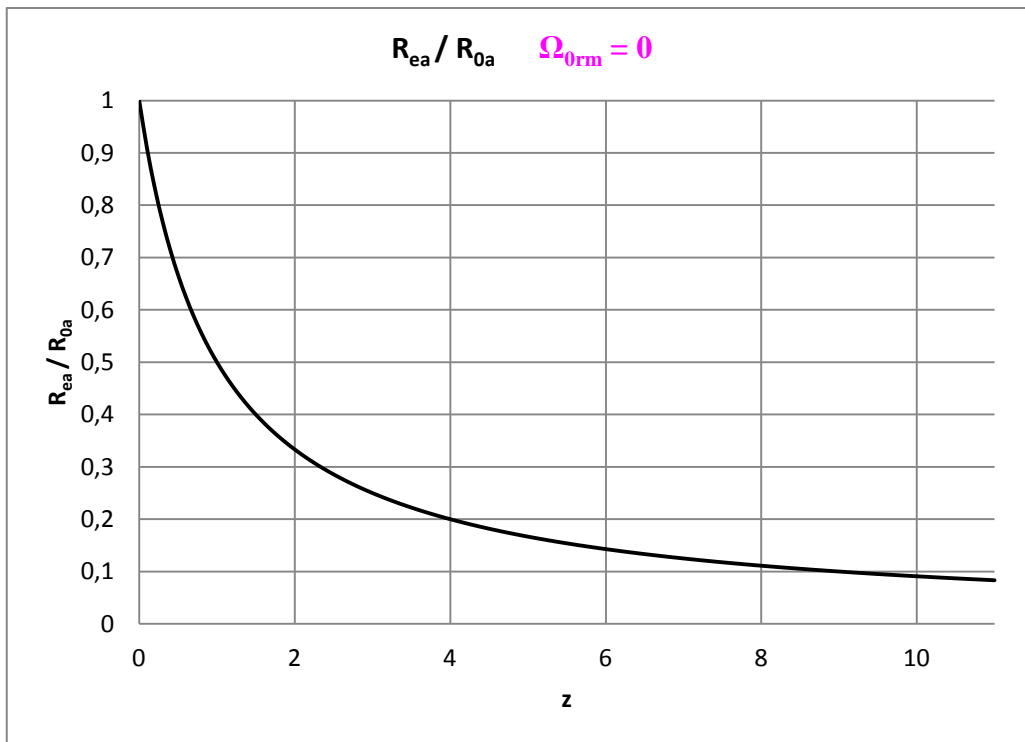


Figure 4. Redshift distance R_{ea} normalized to the distance R_{0a} and $\Omega_{0rm} = 0$.

This distance is not depending on parameter β_{0m} .

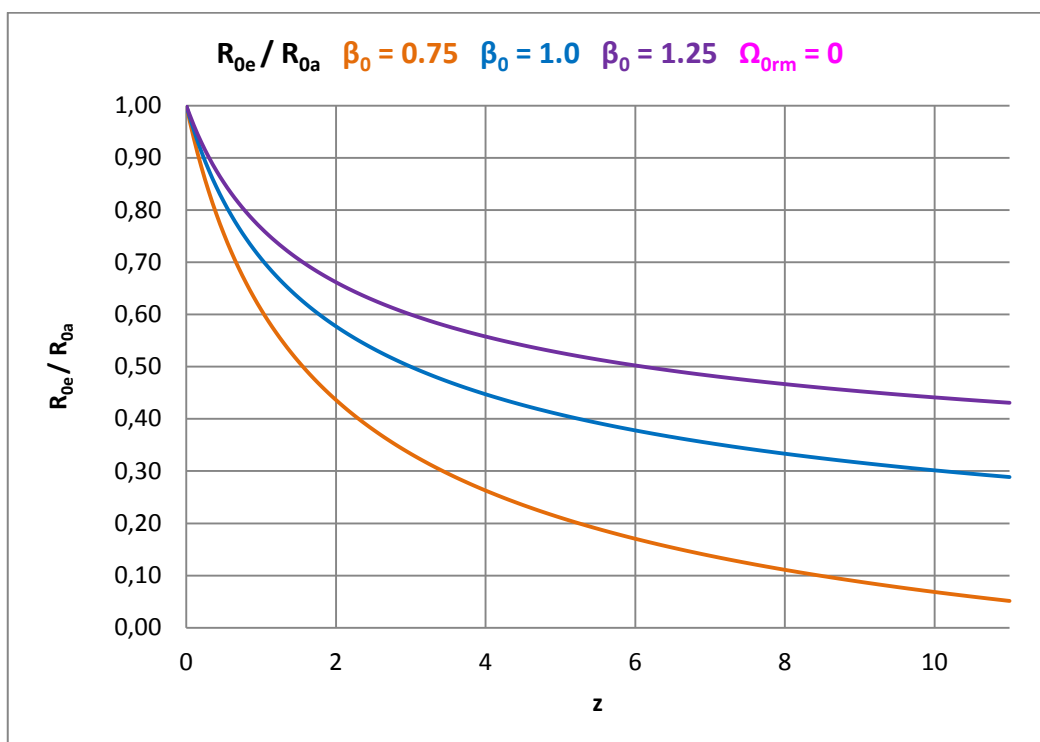


Figure 5. Redshift distance R_{0e} normalized to the distance R_{0a} for various values of the parameter β_{0m} and $\Omega_{0m} = 0$.

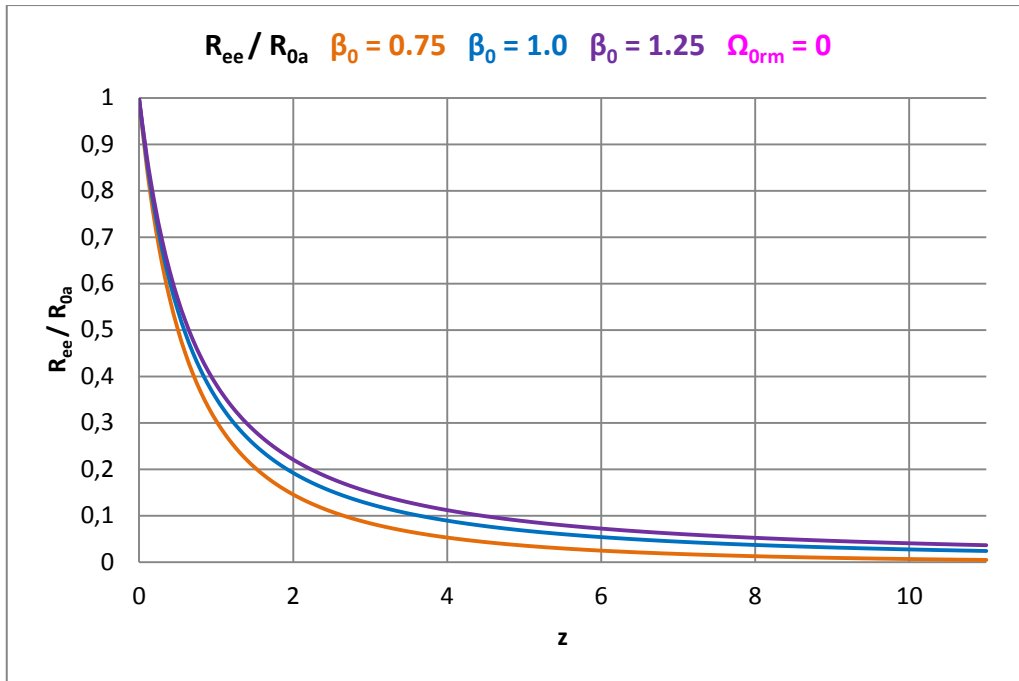


Figure 6. Redshift distance R_{ee} normalized to the distance R_{0a} for different values of the parameter β_{0m} and $\Omega_{0m} = 0$.

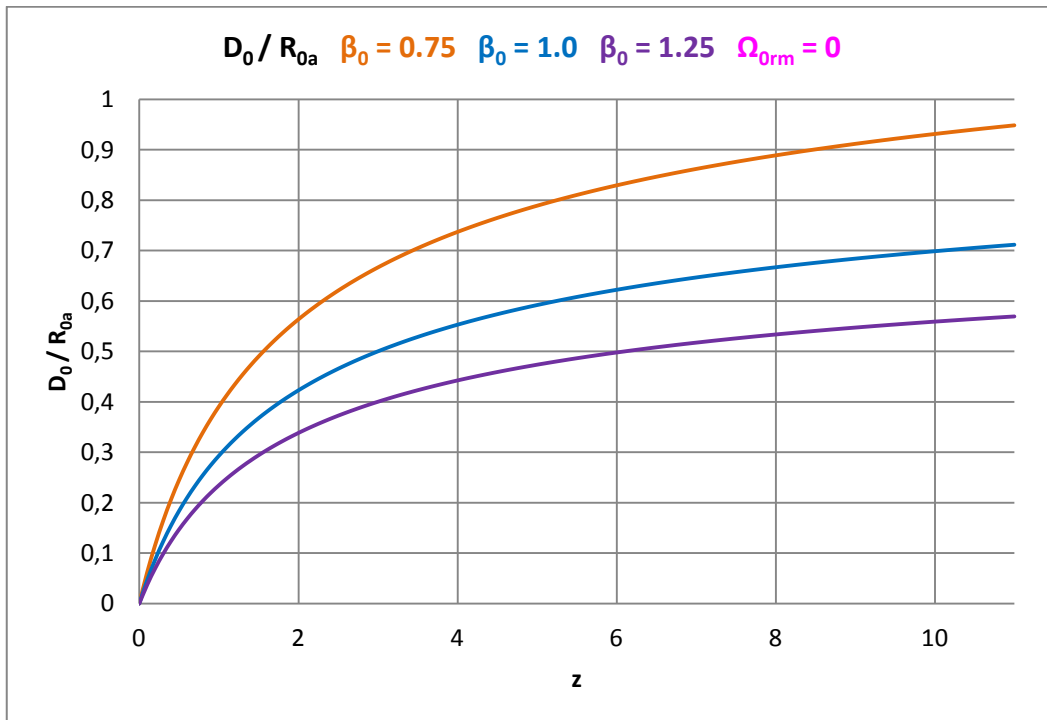


Figure 7. Today's redshift distance D_0 normalized to the distance R_{0a} for various values of the parameter β_{0m} and $\Omega_{0rm} = 0$.

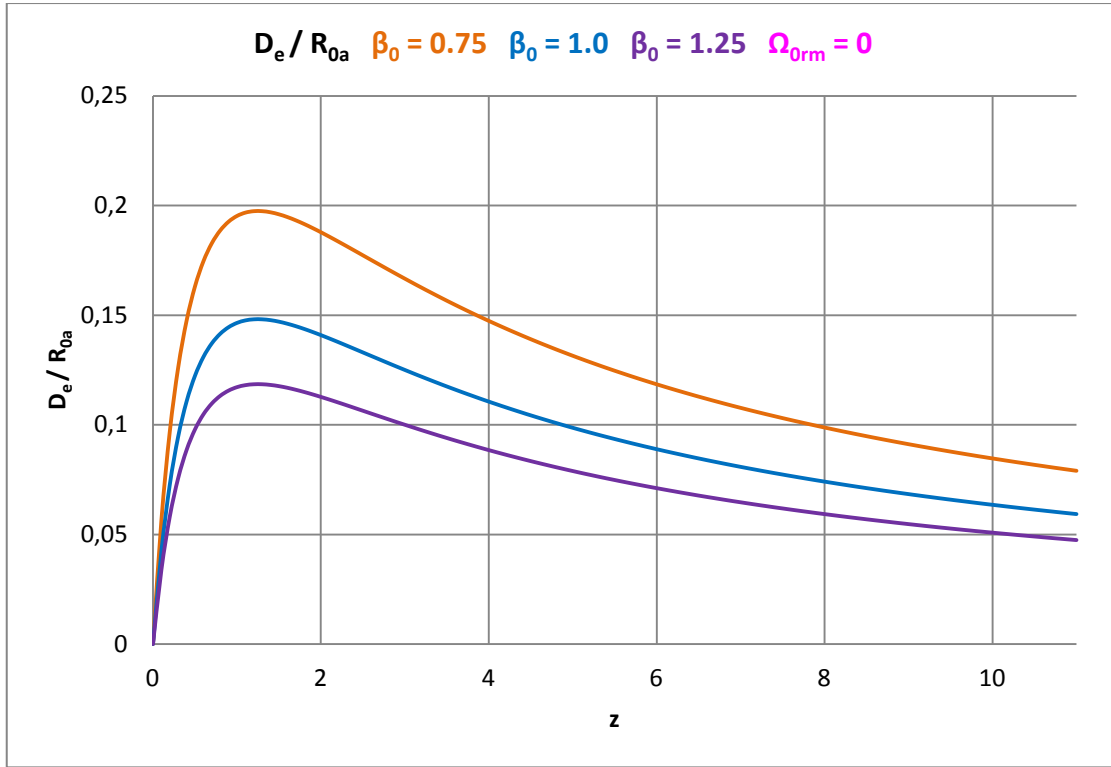


Figure 8. The redshift distance at that time D_e normalized to the distance R_{0a} for various values of the parameter β_{0m} and $\Omega_{0rm} = 0$.

In the specialist literature, none of these redshift distances are known and they cannot be derived there, respectively.

We will give concrete values for such redshift distances for the galaxy M87 and 27 SN Ia below.

4. Determination of the parameter values

The present paper presents a theoretical derivation of redshift distances, which is done without approximations for e.g. small redshifts z and is mainly of theoretical nature. The essay is therefore a theoretical offer to the observing cosmologists.

Nevertheless, in this chapter we will apply the theory presented here in detail to some measurement results of observational cosmology, whereby we only demonstrate the principle of evaluating the measurement data. For this reason, no more detailed error analyzes are carried out. We leave that to the experts of observational cosmology.

4.1 Magnitude-redshift relation

The apparent magnitude m depends according to Eq. (39) in addition to the measurable redshift z also on the three parameters β_{0m} , Ω_{0rm} and m_{0a} .

To find the values of the parameters, the quasar catalog by Véron-Cetty et al. [1] is suitable in which measured redshifts and apparent magnitudes of 132,975 quasars are given.

Fig. 9 shows all these quasars in a single magnitude-redshift diagram, where we have used $\log_{10}(cz)$ on the axis of ordinates.

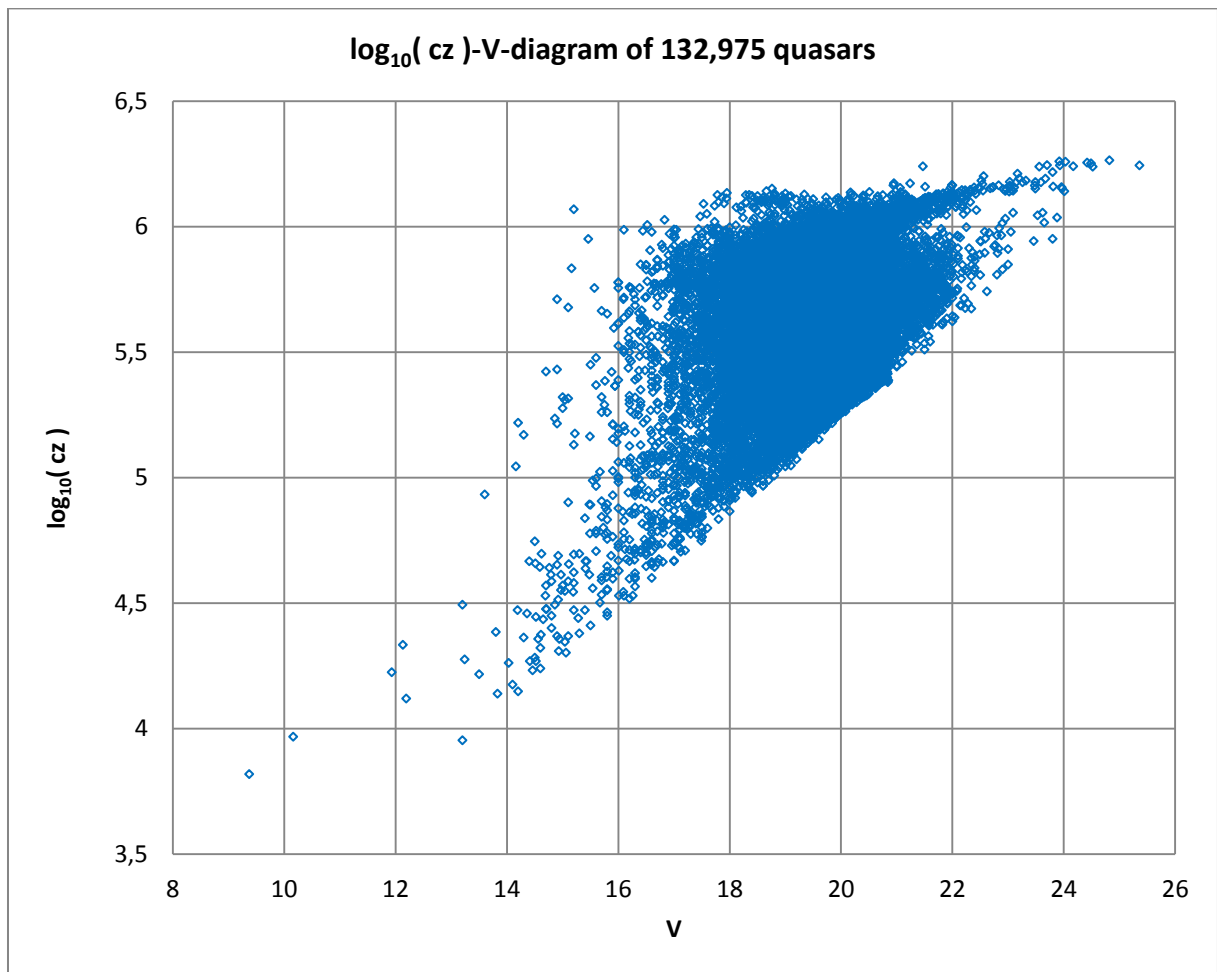


Figure 9. Magnitude-redshift diagram for all 132,975 quasars according to M.-P. Véron-Cetty et al. [1].

A clear edge exists on the right side of the accumulation of measurement points, which indicates minimum apparent magnitudes for associated redshifts. The apparent magnitudes are usually up to far to the left of this edge in the diagram.

If we form redshift intervals with mean values of the redshifts and the corresponding mean values for the apparent magnitude, this fact leads to a clear curvature of the mean value curve in the direction of the redshift axis. This curvature should be explained by means of a valid astrophysical theory. More precisely: The theory has to explain the curvature! This suggests that our redshift distance [i.e. ultimately Eq. (39)] could be suitable for the measured values.

It is precisely this strange magnitude-redshift diagram, which was stimulating us to think about cosmological distance determinations for many years [9].

To evaluate the quasar data set, we first create 75 z-intervals with 1,773 quasars each. For these intervals, we calculate the mean values $\langle z_i \rangle$ and the associated mean values $\langle m_i \rangle$ of the quasars.

We use the following χ^2 -function

$$\chi^2(p_k) = \frac{1}{(N-1)} \sum_{i=1}^N [m_{th,i}(p_k) - m_{obs,i}]^2 \quad (57)$$

for the evaluation.

The abbreviation p_k with $k = 1, 2, 3$ stands for the three parameters we are looking for, β_{0m} , Ω_{0rm} and m_{0a} .

If we use our magnitude-redshift relation (39), the result is more concrete

$$\chi^2(\beta_{0m}, m_{0a}, \Omega_{0rm}) = \frac{1}{(N-1)} \sum_{i=1}^N \left[5 \log_{10} \left\{ \frac{1}{\beta_{0m}} \left[\sqrt{1 + \Omega_{0rm}} - \sqrt{\Omega_{0rm} + \frac{1}{(1+z)}} \right] + z \right\} - 5 \log_{10}(1+z) + m_{0a} - m_{obs,i} \right]^2 \quad (57a)$$

Using the quasar data and the usual mathematical procedure, we find the parameters to be $\beta_{0m} = 1.05401$ and $m_{0a} = 20.30342$.

Fig. 10 shows the result of the mean value formation and the adaptation of the theory to the curvature of the mean value curve.

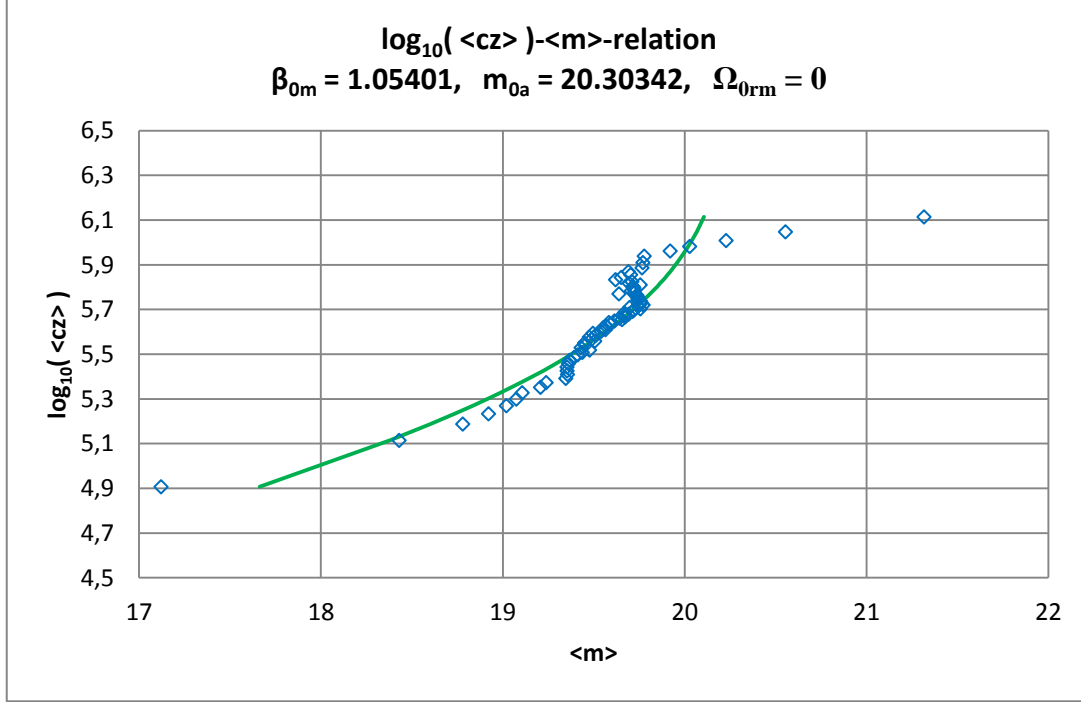


Figure 10. Magnitude-redshift diagram for 132,975 quasars according to M.-P. Véron-Cetty et al. [1].

To interpret the measured magnitude-redshift relation:

From our point of view, the quasars came in to being historically slowly as relatively few and weakly luminous objects at a point in time that corresponds to about $z \approx 4.3$ (development effect). The quasars later behaved as our theory expects in flat space and moved with time - i.e. for decreasing redshifts z - on average along the theoretical curve (in the diagram from top right diagonally to bottom left). The quasars have gradually died out in the recent past and became relatively bright in this process.

4.2 Number-redshift relation

We use the following variance to evaluate the number-redshift relation

$$\chi^2(p_k) = \frac{1}{(N-1)} \sum_{i=1}^N [N_{th,i}(p_k) - N_{obs,i}]^2 \quad (58)$$

The abbreviation p_k with $k = 1, 2, 3$ stands for the three parameters we are looking for, β_{0m} , Ω_{0rm} and N_{0a} .

If we insert our number-redshift relation (47), the Eq. (58) is concrete

$$\chi^2(\beta_{0m}, N_{0a}, \Omega_{0rm}) = \frac{1}{(N-1)} \sum_{i=1}^N \left[3 \log_{10} \left\{ \frac{1}{\beta_{0m}} \left[\sqrt{1 + \Omega_{0rm}} - \sqrt{\Omega_{0rm} + \frac{1}{(1+z)}} \right] + z \right\} - 3 \log_{10}(1+z) + \log_{10} N_{0a} - N_{obs,i} \right]^2 \quad (58a)$$

Using simple mathematics, we find $N_{0a} = 172,376$ for the theoretically expected total number of quasars, if we use the value $\beta_{0m} = 1.05401$ found via the magnitude-redshift relation.

The expected number N_{0a} is slightly larger than the actual number of quasars measured within the catalogue of M.-P. Véron-Cetty et al. [1]. This indicates a certain incompleteness of the measurements, because N_{0m} means the sum of all objects which should be found up to $z = \infty$ (see chapter 2.6). May be that development effects have to be involved also, but such effects are not the object of our theoretical contemplations.

Fig. 11 shows the graphic result.

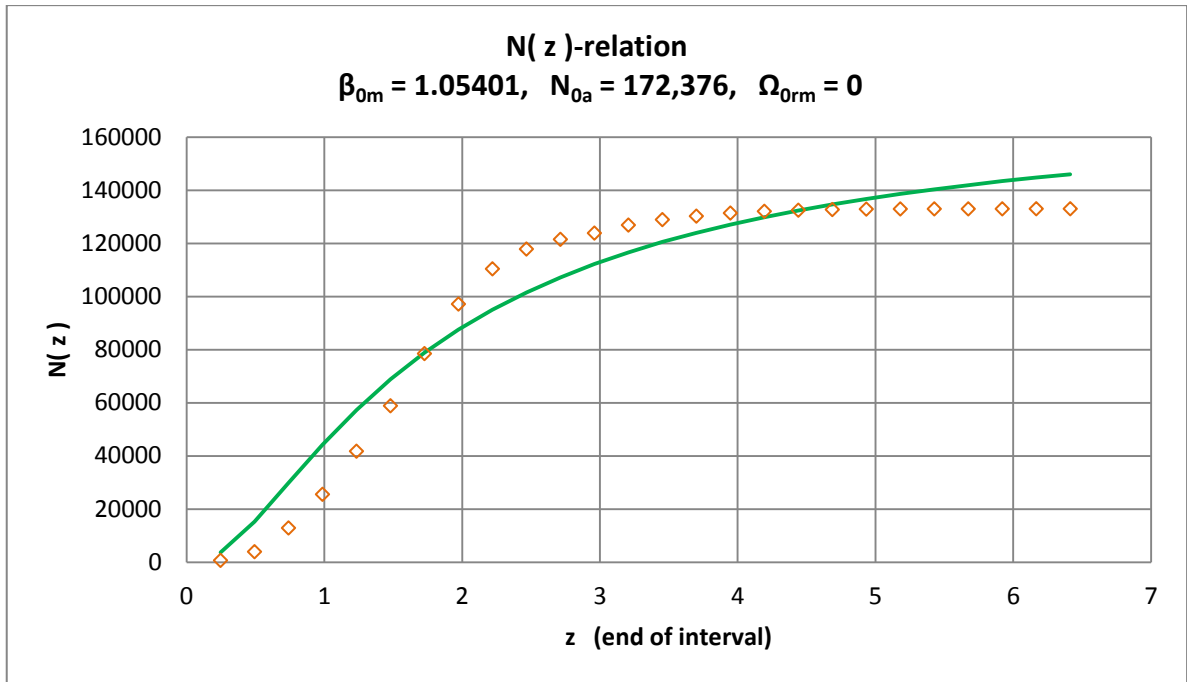


Figure 11. Number-redshift diagram for the 132,975 quasars according to M.-P. Véron-Cetty et al. [1].

4.3 Angular size-redshift relation

In this case, we use the measurement data from K. Nilsson et al. [2] to find an average linear size of the cosmic objects measured there.

The starting point is the variance

$$\chi_{\varphi}^2(p_k) = \frac{1}{(N-1)} \sum_{i=1}^N [\varphi_{th,i}(p_k) - \varphi_{obs,i}]^2 \quad . \quad (59)$$

The abbreviation p_k with $k = 1, 2, 3$ stands for the three parameters we are looking for, β_{0m} , Ω_{0rm} and δ/R_{0a} .

If we use our angular size-redshift relation (41), the Eq. (59) is concrete

$$\chi_\varphi^2 \left(\frac{\delta}{R_{0a}}, \beta_{0m}, \Omega_{0rm} \right) = \frac{1}{(N-1)} \sum_{i=1}^N \left[\frac{\delta}{R_{0a}} \frac{(1+z)}{\left\{ \frac{1}{\beta_{0m}} \left[\sqrt{1+\Omega_{0rm}} - \sqrt{\Omega_{0rm} + \frac{1}{(1+z)}} \right] + z \right\}} - \varphi_{obs,i} \right]^2 \quad (59a)$$

The comparison of the theory with the measurement data using $\beta_{0m} = 1.05401$ results in a value of $\delta/R_{0a} = 5.46 \times 10^{-5}$.

Fig. 12 shows the graphic result.

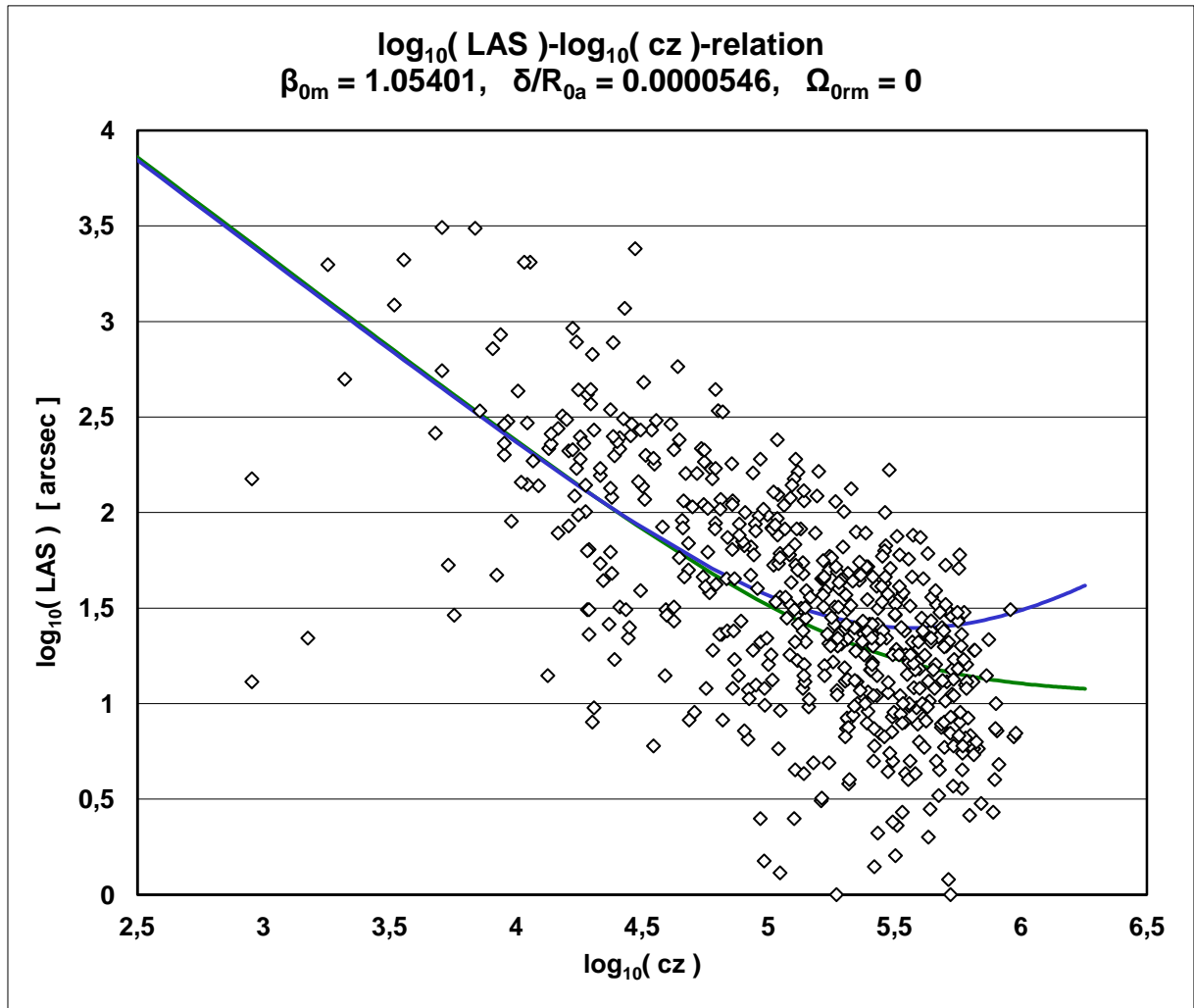


Figure 12. Angular size-redshift diagram according to K. Nilsson et al. [2].

For the purpose of comparison, the theoretical curve from the literature [see Eq. (67)] was inserted also. This curve cannot explain the position of the measured values in the diagram especially for larger redshifts.

The determination of the linear size δ requires the knowledge of R_{0a} . Because the absolute magnitudes are known for some SN Ia (which differ strangely enough slightly from one another), we can determine R_{0a} using a magnitude-redshift diagram of these cosmic objects. We will do that in the next chapter.

4.4 Fixing of R_{0a} with the help of SN Ia

By W. L. Freedman et al. [3], data from a total of 27 SN Ia were made available, with the help of which we can determine both the distance R_{0a} - a current physical distance - and, as a main result, the today's Hubble parameter H_{0a} .

The data we are interested in are the distance modules (μ_{TRGB} and μ_{Ceph} , respectively), the maximum apparent magnitudes (m_{CSP_B0} and m_{SC_B} , respectively) and the radial velocities V_{NED} , from which the redshifts z_{NED} can be calculated.

The methods taken into account in [3] for determining the maximum apparent magnitude and thus the associated absolute magnitude are different, which is why somewhat different values are given for one and the same SN Ia. For our purposes, we calculate the mean values from these data and assign them to the relevant SN Ia.

We calculate the absolute magnitudes M_i of the SN Ia_{*i*} using ($\mu_{\text{TRGB}} - m_{\text{CSP}_B0}$) and ($\mu_{\text{Ceph}} - m_{\text{SC}_B}$), respectively, and then always calculate an average value $\langle M_i \rangle$ if both value pairs are specified for one and the same SN Ia. From all the absolute magnitudes obtained in this way, we finally form the mean value of the absolute magnitude to be $\langle M \rangle \approx -19.245$, which enables us to determine the distance R_{0a} with the aid of the parameter m_{0a} , which results from the magnitude-redshift diagram of the SN Ia. The simple equation for this is

$$R_{0a} = 10^{\frac{(m_{0a} - M)}{5} + 1} . \quad (60)$$

The graphic result is shown in Fig. 13.

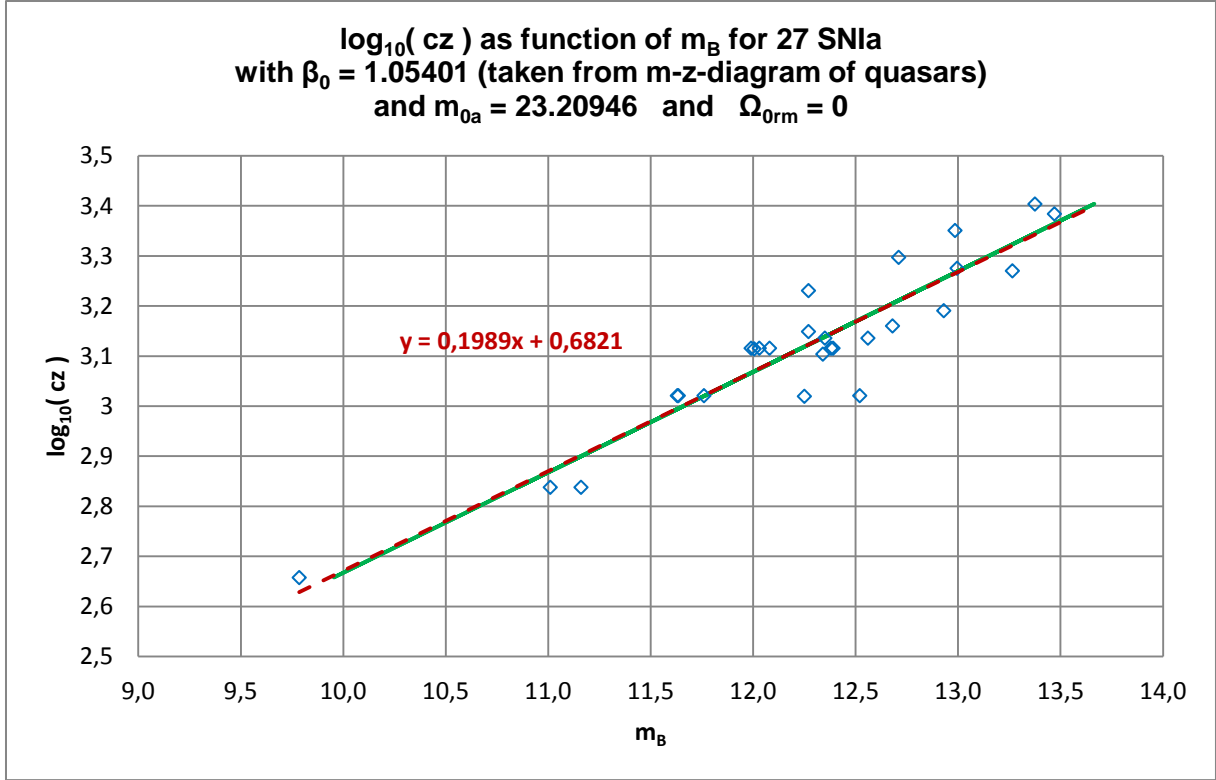


Figure 13. Magnitude-redshift diagram for 27 SN Ia according to W. L. Freedman et al. [3].

The theoretical curve (green) lies exactly on the linear trend line (dashed in red), the equation of which is given in the figure.

Finding $m_{0a} \approx 23.209$ and using the mean value of the absolute brightness $\langle M \rangle = -19.245$, the distance $R_{0a} \approx 3,096.92$ Mpc we are ultimately looking for is the essential result of this data analysis.

With the help of the value of R_{0a} and taking the equation (34), which is an approximation for small redshifts, the today's Hubble parameter $H_{0a} \approx 65.66$ km/(s·Mpc) results, if we neglect the radiation how before also. This value is slightly below the Planck value (2018) with $H_{0, \text{Planck}} \approx 67.66$ km/(s·Mpc) [4].

In Table 9 in the appendix, all the values we have used for the magnitude-redshift diagram of the 27 SN Ia are compiled.

Using equation (24a) we get as result for the today's mass density

$$\rho_{0m} = \frac{3}{2\pi G} \frac{c_0^2}{R_{0a}^2} \beta_{0m}^2 \quad . \quad (61)$$

With the help of parameters, β_{0m} and R_{0a} determined by us, we find $\rho_{0m} \approx 7.822 \times 10^{-29}$ g/cm³ for today's matter density in the universe.

Via

$$M_{F_s} = \frac{4\pi}{3} R_{0a}^3 \rho_{0m} = \frac{2c_0^2}{G} \beta_{0m}^2 R_{0a} \quad (62)$$

the constant mass of the Friedmann sphere results in $M_{F_s} \approx 2.86 \times 10^{56}$ g.

Because we generally do not consider the accuracy here, we simply specify the decimal places with up to three places, whereby the mathematical analysis of the data usually delivers more decimal digits.

Using Eq. (30) we find for the Schwarzschild radius $R_S \approx 13,761.94$ Mpc and the speed which is contained in Eq. (24) results in $V_0 \approx 315,984.25$ km/s. This value is a little bit bigger than the velocity of light c_0 in vacuum. Therefore we could think that the parameter value $\beta_{0m} = 1$ should be realized in the nature. We believe that more and better data material would give us this value.

With the known value $R_{0a} \approx 3,096.92$ Mpc we can calculate the mean linear size of the Nilsson objects [2] to be $\delta \approx 0.169$ Mpc, because we have found $\delta/R_{0a} = 5.46 \times 10^{-5}$ for them.

Using known R_{0a} and β_{0m} , of course, all linear dimensions of these objects can be calculated using their angular size and redshift if they could be measured.

4.5 Calculation of the further redshift distances for the SN Ia and M87

Because we were able to determine R_{0a} , we can graphically display all the further redshift distances in a form, which is not normalized to R_{0a} . The result is shown in Fig. 14, using the values we found for β_{0m} and R_{0a} .

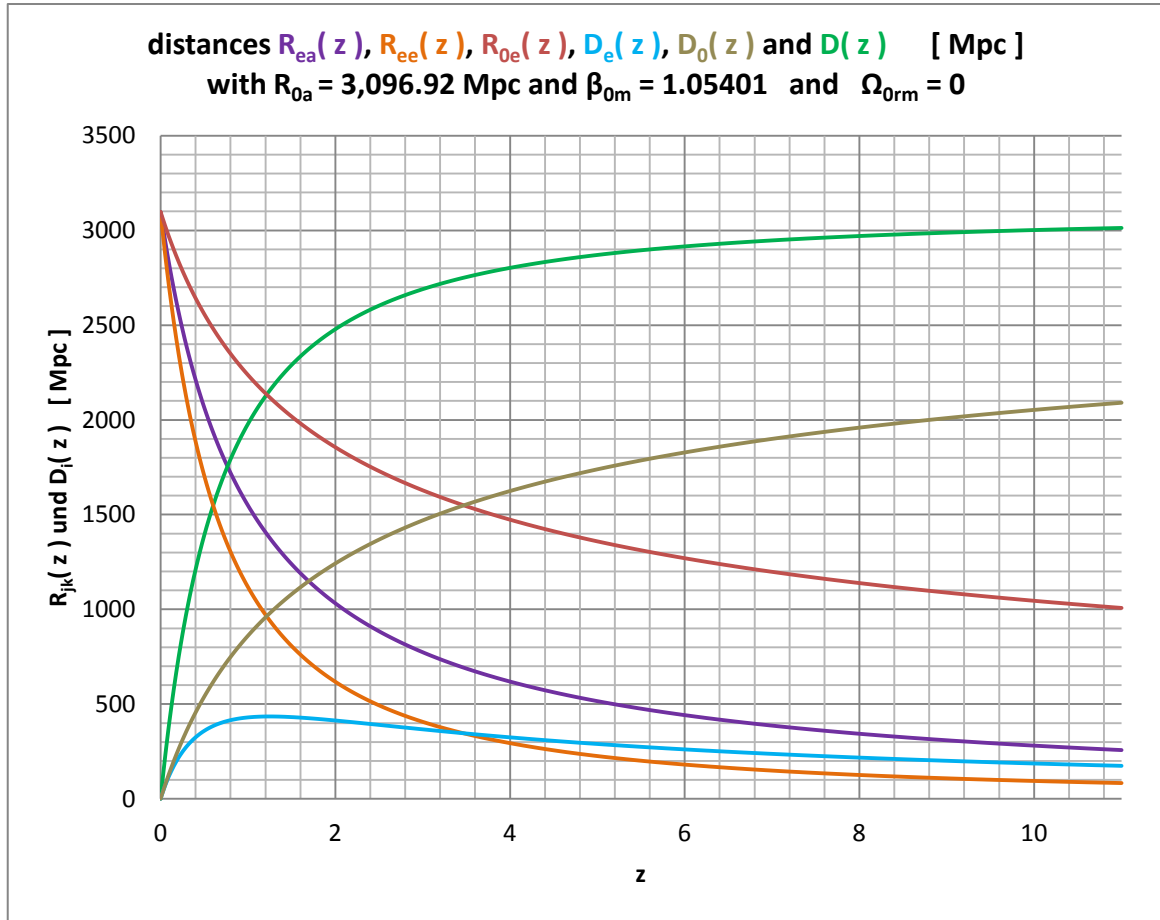


Figure 14. Redshift distance D (real light path) and all further redshift distances D_i ($i = 0, e$) and R_{jk} ($j = 0, e; k = e, a$) as a function of the redshift up to $z = 11$.

To interpret Fig. 14:

a) For D going to R_{0a} the redshift z goes towards infinity. This means that no observer can observe objects for which is $D > R_{0a} \approx 3,096.92$ Mpc.

b) The light path distance $D = R_{0a} - R_{ee}$ is always greater than the distances D_0 (today's) and D_e (time at that time).

In particular, the light path D is not equal to the today's distance D_0 between two astrophysical objects.

c) The distances R_{jk} are physical distances from a coordinate origin and develop directly with the change in the scale parameter $a(t)$ over time. For large redshifts, the scale parameter was correspondingly small and, as a result, the associated distances were also correspondingly small.

d) The distance at that time D_e is interesting: It shows a maximum for a specific redshift and only approaches zero for very large redshifts.

Table 1 summarizes all calculated redshift distances of the 27 SN Ia used by us.

SN Ia	R_{ea}	R_{ee}	R_{0e}	R_{0a}	D_e	D_0	D
1980N	3,083.49	3,074.33	3,087.72	3,096.92	9.16	9.20	22.59

1981B	3,086.11	3,078.74	3,089.52	3,096.92	7.37	7.40	18.18
1981D	3,083.49	3,074.33	3,087.72	3,096.92	9.16	9.20	22.59
1989B	3,089.82	3,084.97	3,092.06	3,096.92	4.85	4.86	11.95
1990N	3,086.11	3,078.74	3,089.52	3,096.92	7.37	7.40	18.18
1994D	3,086.11	3,078.74	3,089.52	3,096.92	7.37	7.40	18.18
1994ae	3,080.97	3,070.11	3,086.00	3,096.92	10.87	10.92	26.81
1995al	3,077.56	3,064.38	3,083.66	3,096.92	13.18	13.26	32.54
1998aq	3,082.85	3,073.27	3,087.29	3,096.92	9.59	9.63	23.65
1998bu	3,089.82	3,084.97	3,092.06	3,096.92	4.85	4.86	11.95
2001el	3,086.14	3,078.79	3,089.54	3,096.92	7.35	7.38	18.13
2002fk	3,077.78	3,064.76	3,083.81	3,096.92	13.03	13.11	32.16
2003du	3,072.10	3,055.23	3,079.91	3,096.92	16.87	17.01	41.69
2005cf	3,073.91	3,058.27	3,081.16	3,096.92	15.65	15.76	38.66
2006dd	3,083.49	3,074.33	3,087.72	3,096.92	9.16	9.20	22.59
2007af	3,076.57	3,062.72	3,082.98	3,096.92	13.85	13.94	34.20
2007on	3,083.49	3,074.33	3,087.72	3,096.92	9.16	9.20	22.59
2007sr	3,079.44	3,067.53	3,084.95	3,096.92	11.90	11.97	29.39
2009ig	3,070.96	3,053.32	3,079.13	3,096.92	17.64	17.79	43.60
2011by	3,082.85	3,073.27	3,087.29	3,096.92	9.59	9.63	23.65
2011fe	3,092.23	3,089.02	3,093.71	3,096.92	3.21	3.21	7.90
2011iv	3,083.49	3,074.33	3,087.72	3,096.92	9.16	9.20	22.59
2012cg	3,086.11	3,078.74	3,089.52	3,096.92	7.37	7.40	18.18
2012fr	3,083.53	3,074.40	3,087.75	3,096.92	9.13	9.17	22.52
2012ht	3,082.04	3,071.91	3,086.74	3,096.92	10.14	10.19	25.01
2013dy	3,082.42	3,072.54	3,086.99	3,096.92	9.88	9.93	24.38
2015F	3,083.85	3,074.93	3,087.97	3,096.92	8.91	8.95	21.99

Table 1. Redshift distance D and the further redshift distances D_i and R_{jk} of all 27 SN Ia.

To interpret the distances from Table 1:

For a more detailed explanation, we take into account the SN Ia **2006dd**, for example, and use it to interpret the meaning of the distances in the table.

The "light-travel time" always means the time interval between the emission of light (the time at that time t_e , **2006dd**) by the SN Ia **2006dd** and today (t_0), i.e. $\Delta t = t_0 - t_e$, **2006dd**. This light-travel time is generally different for all observable cosmic objects, here especially for the individual SN Ia **2006dd** we will consider.

- a) The today's (t_0) distance between the selected SN Ia **2006dd** and us as observers is $D_0 \approx 9.20$ Mpc.
- b) The distance at that time (t_e) between this SN Ia **2006dd** and us as observers was $D_e \approx 9.16$ Mpc.

According to this, the distance between the two cosmic objects has increased by about 0.04 Mpc during the light-travel time $\Delta t = t_0 - t_e$, 2006dd.

c) The SN Ia 2006dd has been shifted expansively away from the origin of the coordinates by $\Delta R_e = R_{0e} - R_{ee} \approx 13.393$ Mpc during the light-travel time due to the time-dependent scale parameter $a(t)$.

d) The galaxy with us as observers has been expansively shifted away from the origin of the coordinates by $\Delta R_a = R_{0a} - R_{ea} \approx 13.433$ Mpc during the light-travel time due to $a(t)$.

The difference between the two displacement distances is of course the increase in the distance between the two cosmic objects noted above.

e) The real light path (redshift distance) covered by the photons within the time $\Delta t = t_0 - t_e$, 2006dd is $D \approx 22.59$ Mpc. It is unequal to the other mentioned distances D_i and greater than these.

4.6 Evaluation of the data from the black hole in M87

For the sake of simplicity, we summarize the data taken from the specialist literature on the galaxy M87 containing a black hole (BH) in it in the first line of Table 2 {see [5] and [6]}.

The second line lists the data specified in this paper, which usually differ from those in the literature.

	D [Mpc]	M_B [mag]	z	m_B [mag]	Θ_{BH} [μas]	δ/2 = R_S [pc]	M_{BH} [g]
literature	16.9 / 16.8	-23.5	0.004283	9.6	42		1.2928E+43
we	19.45	-21.845				0.11348	2.3583E+45

Table 2. Summary of data from galaxy M87 containing a black hole in it.

The theory was adapted to the measured angle size Θ_{BH} from the literature. Overall, a larger redshift distance D , a smaller absolute magnitude M_B and a significantly larger mass M_{BH} of the black hole follow.

Table 3 lists the values found by means of our theory for all redshift distances R_{jk} , D_i and D , respectively.

[Mpc]	R_{ea}	R_{ee}	R_{0e}	R_{0a}	D_e	D₀	D
we	3,083.71	3,077.47	3,090.65	3,096.92	6.25	6.27	19.45
literature	---	---	---	---	---	---	16.8

Table 3. Redshift distances D_i , D and R_{jk} belonging to the black hole in M87.

From these values, the expansion-related shifts in distance of the galaxy M87 and of the galaxy with us as observers can be calculated, which took place during the time of light travel.

The theory from the specialist literature does not know the first five distances listed in Table 3. It can therefore not be calculated using this theory and not determine in terms of value.

The distance D differs because of the physical meaning: In our theory, D is the real physical light path, which is not the case in the astrophysical literature.

We briefly interpret the meaning of the distances listed in Table 3, whereby the light-travel time is again defined as above described:

- a) The today's (t_0) distance between the BH or the galaxy M87 and us as observers is $D_0 \approx 6.27$ Mpc.
 - b) The distance at that time (t_e) between the BH (or M87) and us as observers was $D_e \approx 6.25$ Mpc.
- Accordingly, the distance between the two cosmic objects has increased by about 0.02 Mpc during the light-travel time $\Delta t = t_0 - t_{e, \text{BH, M87}}$.
- c) The BH (or M87) has been shifted expansively away from the origin of the coordinates by $\Delta R_e = R_{0e} - R_{ee} \approx 13.18$ Mpc during the light-travel time due to the time-dependent scale parameter $a(t)$.
 - d) The galaxy with us as observer was expansively shifted away from the origin of the coordinates by $\Delta R_a = R_{0a} - R_{ea} \approx 13.21$ Mpc during the light-travel time due to $a(t)$.
 - e) The real light path (redshift distance) covered by the photons during the time $\Delta t = t_0 - t_{e, \text{BH, M87}}$ is $D \approx 19.45$ Mpc. It is unequal to the other mentioned distances D_i and greater than these.

Fig. 15 shows the various calculated distances in a clear form.

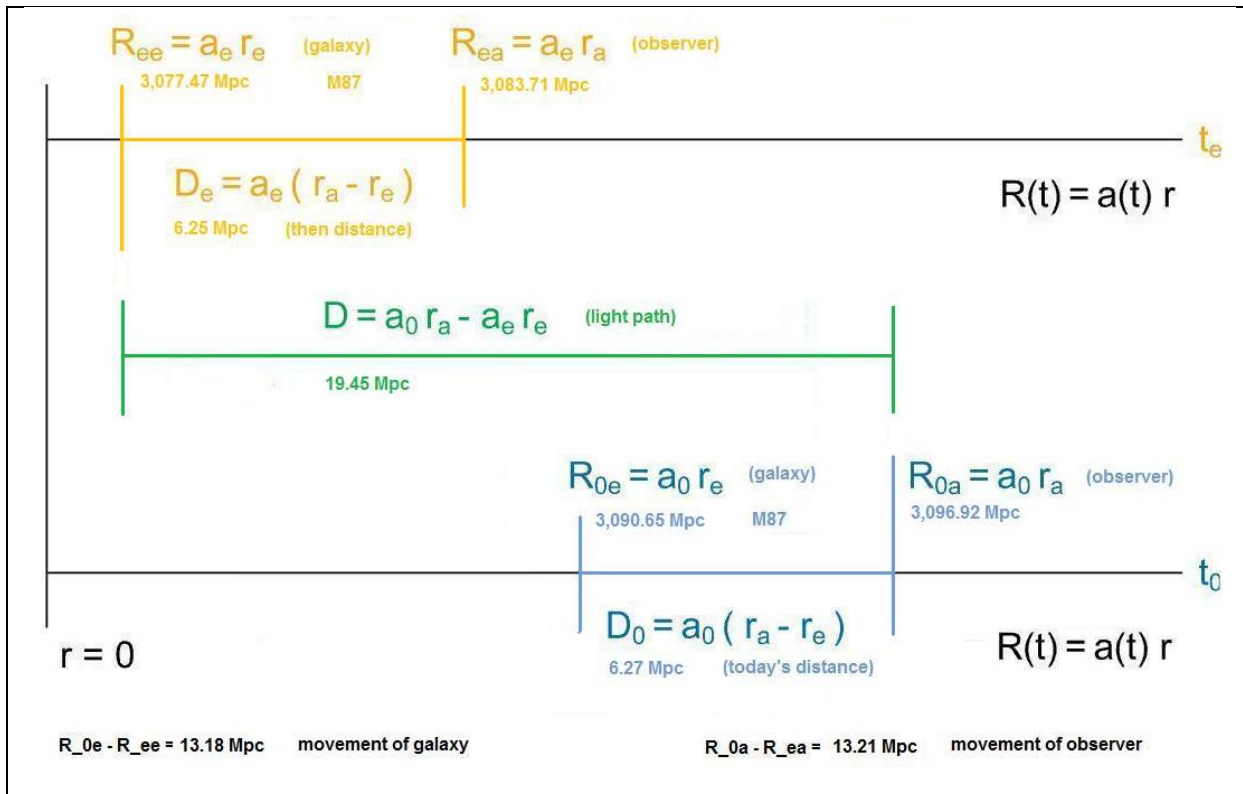


Figure 15. Visualization of the distances D_i , D and R_{jk} with regard to M87 and observer.

The distances are not drawn to scale here.

4.7 Maximum values known today: Galaxy UDFj-39546284 and Quasar J0313

The galaxy UDFj-39546284 [8] currently holds the record among the galaxies with a redshift of $z = 10.3$, while the quasar J0313 [7] with $z = 7.642$ holds the analog record among the quasars.

Table 4 shows the corresponding distances R_{jk} , D_i and D together using Mpc as unit of measurement.

object name	z	D	D_0	D_e	R_{ee}	R_{0e}	R_{ea}	R_{0a}	object
J0313	7.642	2,962.902	2,043.448	236.455	134.018	1,158.183	358.357	3,096.92	quasar
UDFj-39546284	10.300	3,005.525	2,175.642	192.535	91.395	1,032.763	274.064	3,096.92	galaxy

Table 4. All calculated redshift distances R_{jk} , D_i and D for the two cosmic objects with the maximum redshifts.

Table 5 summarizes the spatial shifts of the objects with respect to the coordinate origin due to the expansion during the associated light travel times.

object name	$R_{0e} - R_{ee}$	$R_{0a} - R_{ea}$	object
J0313	1,024.165	2,738.563	quasar
UDFj-39546284	941.368	2,822.856	galaxy

Table 5. Expansion-related shifts in the distance of the quasar and the galaxy [Mpc].

We have already explained above how the tables have to be interpreted.

Fig. 16 shows the distances D_i and D of the three special astrophysical objects analyzed in this paper in a diagram, whereby we have entered all numerical values for the distances in Mpc.

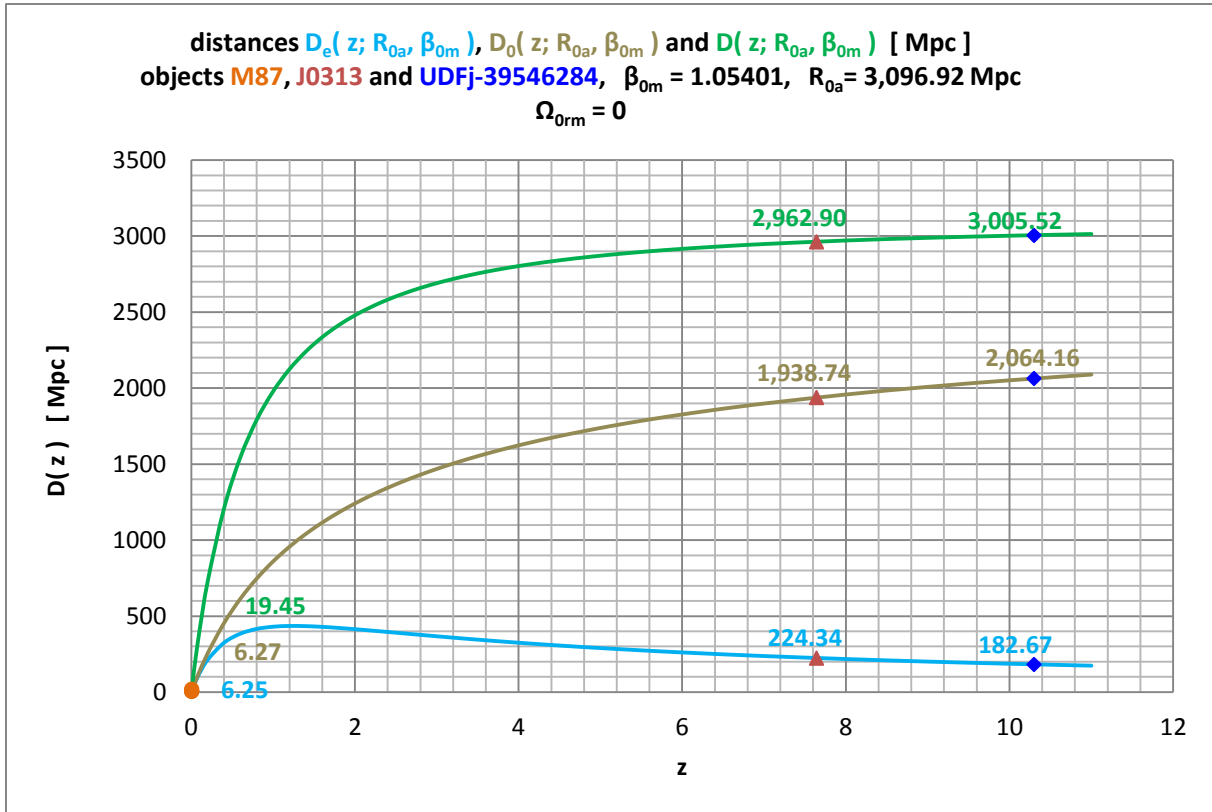


Figure 16. All distances D_i and D for M87, J0313 and UDFj-39546284.

The middle curve shows the current distances D_0 of the three objects from us as observers. These distances are clearly shorter than the associated light paths D of these objects.

5 Additions

5.1 About the mass of Friedmann sphere

The cause of the expansion of the universe visible to us as observers is its constant mass M or the time-varying density $\rho_m(t)$, respectively. It ensures that the scale parameter changes over time. To check this statement, one should simply set the matter density in the Friedmann equation to zero.

Every cosmologist, therefore, has to ask himself where exactly this mass is located in the visible universe. He can gain an answer for this by borrowing the appropriate ideas from classical non-relativistic Newtonian cosmology. There he has to imagine a mass sphere whose radius changes over time (e.g. grows). This means that the mass in question is completely within this sphere, and it is evenly distributed and remains there according to the cosmological principle. In relativistic cosmology, the time depend product of scale parameter and co-moving coordinate distance $R(t) = a(t) r$ takes over the role of the physical radius of the mass sphere, and it holds that the entire mass to be considered is inside this sphere (Friedmann sphere named here).

Incidentally, the Friedmann equation of the flat universe looks strangely exactly as the equation of the non-relativistic Newtonian cosmology. There is no relativity seen in the equation, e.g., in the sense of limiting the rate of change da/dt of the scale parameter to the speed of light c_0 .

The Fig. 17 shows the projection of a Friedmann sphere in to the plane at time t_0 (today) in which examples of possible places for an observer and galaxy observed are drawn.

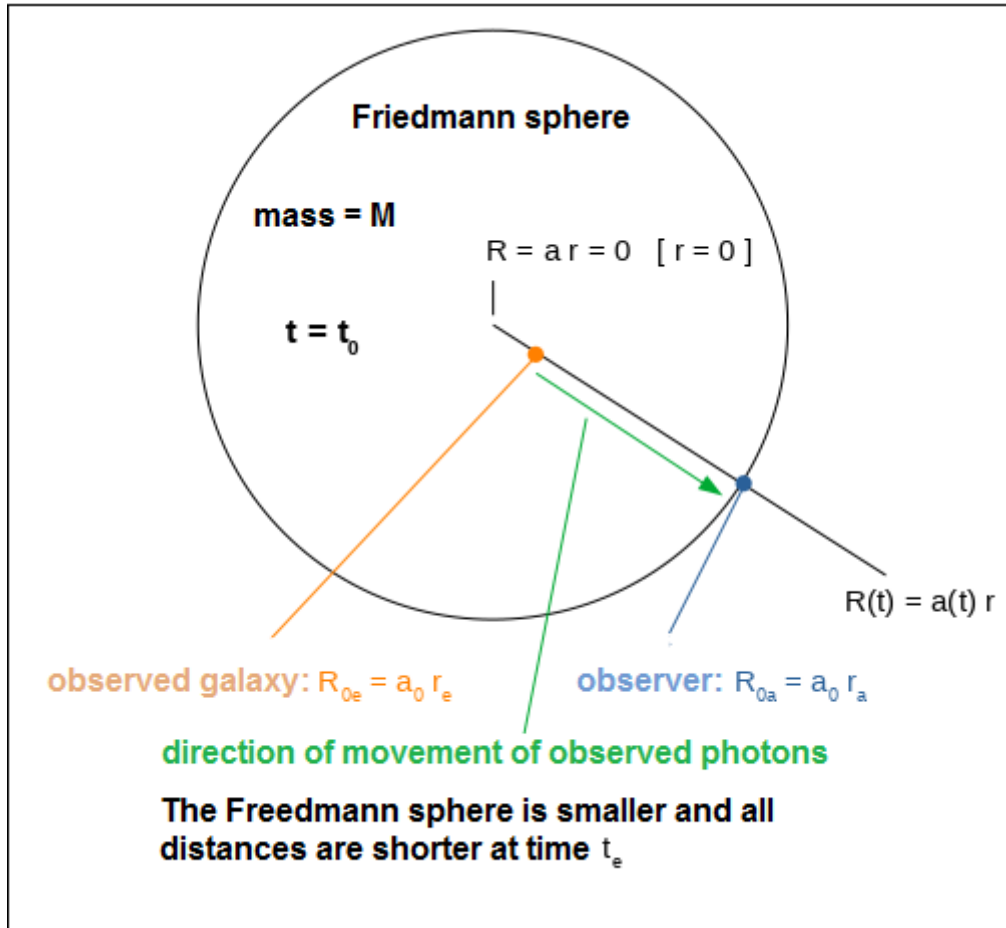


Figure 17. Friedmann sphere containing examples of physical locations of an observer and a galaxy.

Because of the law of conservation of mass

$$M_{Fs} = \frac{4\pi}{3} \rho_{0m} a_0^3 r_a^3 = \frac{4\pi}{3} \rho_{0m} R_{0a}^3 \quad (30)$$

which is used here, we see that R_{0a} is today's radius of the Friedmann sphere with today's mass density ρ_{0m} .

An observable galaxy can minimally have the co-moving coordinate with $r_e = 0$. If a galaxy is placed there, we observe an infinitely large redshift for such a galaxy according to our redshift distance. For all other locations $r_e \neq 0$ of an observed galaxy, a smaller redshift is always measured.

Of course, each observer can also, e.g., look in exactly the opposite direction to the direction shown (green arrow). In this case, he looks again into a Friedmann sphere, which belongs to this direction. For $D = R_{0a}$, there is also an infinite redshift in this direction. The observer can of course also look in any other directions. The observer always looks into Friedmann spheres, which of course partially overlap.

Overall, there is a part of the universe with a spherical radius R_{0a} , that is visible to any observer. A universe thought to be spherical corresponds to at least one sphere with the radius $2xR_{0a}$, since beyond R_{0a} there is always also mass. Every observer sits on the surface of Friedmann spheres. Nevertheless, he can believe that his place is also in a center of such a Friedmann sphere.

If we would put the position of an observer a little outside the Friedmann sphere shown in Fig. 16, he would find the same situation as described above, if the universe would be actually much larger than a sphere with the radius $2 \times R_{0a}$ or even infinitely large.

5.2 About the derivation of the redshift distance in the specialist literature

In the specialist literature, the observer is usually placed in the coordinate origin $r_a = 0$ (see Fig. 18). Because of $r_e \geq r_a = 0$, this results in the light path simply as $D_{literature} = a_0 r_e$. This depends only on the co-moving coordinate location r_e of the observed galaxy and on the today's value of the scale parameter a_0 . An earlier scale parameter such as a_e does not play a role in this approach, which we consider as a strong limitation of the generality.

In this case, the photons run inside a mass sphere from the outside to the inside, i.e., always towards the origin $r_a = 0$ (incoming photons). Any other way of defining $D_{literature}$ would be physically nonsense.

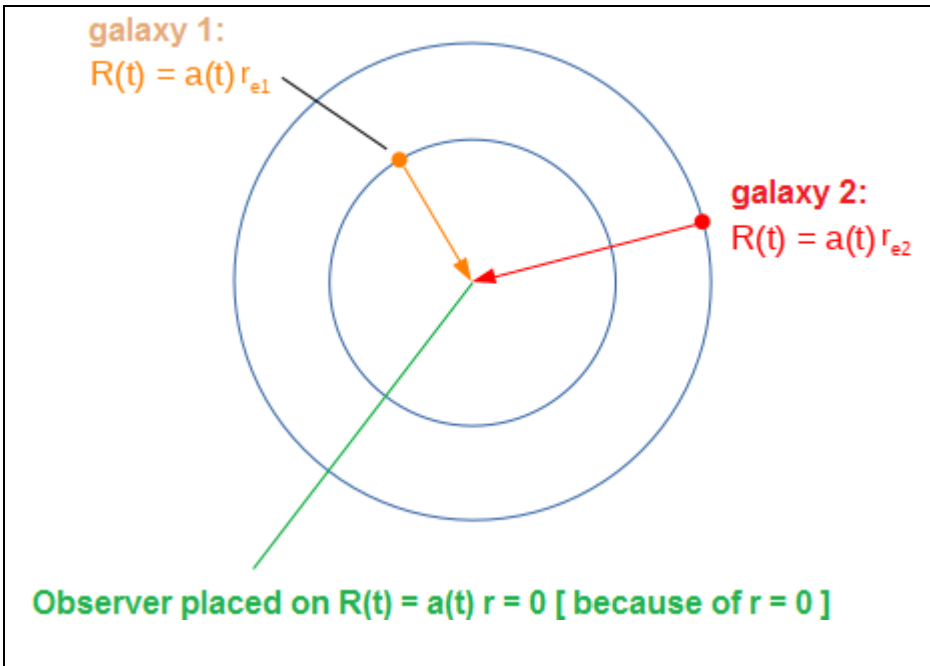


Figure 18. Observer generally placed on the center of the co-moving coordinate system ($r_a = 0$).

The calculation analogous to our derivation of the redshift distance (see chapter 2.2) results (assuming $\Omega_{0\text{rm}} = 0$ here) first in

$$D_{\text{literature}}(z; a_0, R_S) = D_0 \frac{(1+z - \sqrt{1+z})}{(1+z)} \quad \text{with} \quad D_0 = 2a_0 \sqrt{\frac{a_0}{R_S}} . \quad (63)$$

We have denoted the index of the maximum distance for which $z = \infty$ is reached with 0, because the calculation based on $D_{\text{literature}, i} = a_0 r_{e, i}$ generally gives the today's distance between any galaxy i and any observer.

In the specialist literature, the magnitude distance is indicated with

$$D_m = (1+z) D_{\text{literature}} , \quad (64)$$

whereby with the help of factor $(1+z)$ an overall thinning of the number of photons due to the enlargement of the spherical area on which the radiation hits after its way through the universe and the energy loss due to the redshift is taken into consideration.

Therefore, it results first in

$$D_m(z; a_0, R_S) = 2a_0 \sqrt{\frac{a_0}{R_S}} (1+z - \sqrt{1+z}) \quad (65)$$

or

$$D_m(z; a_0, R_S) = 2a_0 \sqrt{\frac{a_0}{R_S}} (1+z) \left(1 - \frac{1}{\sqrt{1+z}}\right) . \quad (65a)$$

Here, too, the prefactor is a distance parameter for which can be introduced an apparent magnitude.

If, in another case which is also possible, the observed galaxy (each one because there are many; see Fig. 19) each placed to its own coordinate origin (outgoing photons), the result of calculation - for obvious reasons of symmetry - is of course the same redshift distance as above. This can easily be checked by means of an elementary calculation.

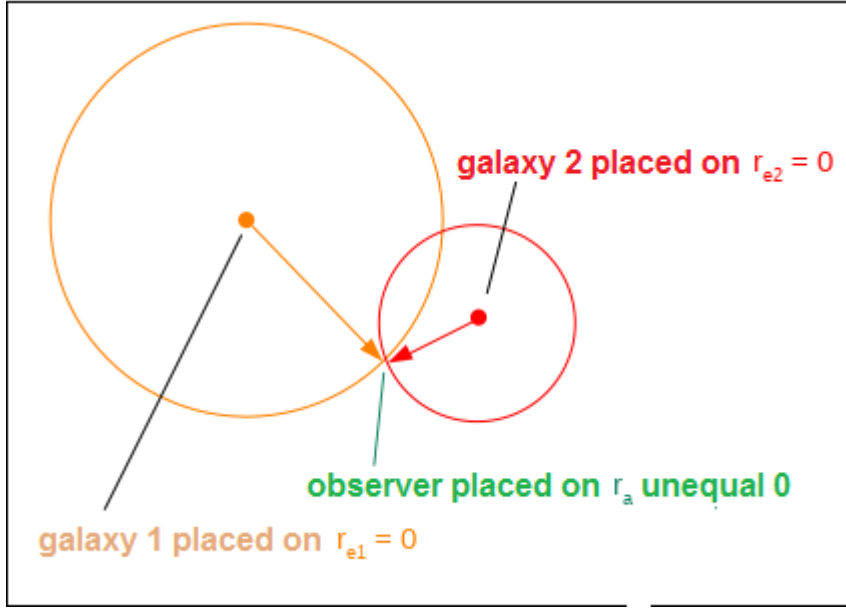


Figure 19. Observed galaxies ($i = 1, 2$) each in their own coordinate origin ($r_{e,i} = 0$).

Therefore, this results in summary for the magnitude-redshift relation in

$$m_{literature}(z; m_{D_0}) = 5 \log_{10} \left(1 - \frac{1}{\sqrt{1+z}} \right) + 5 \log_{10}(1+z) + m_{D_0} \quad . \quad (66)$$

For the angular size-redshift relation we find

$$\log_{10} \varphi_{literature}(z; \delta / D_0) = \log_{10} \frac{\delta}{D_0} - \log_{10}(1+z) - \log_{10} \left(1 - \frac{1}{\sqrt{1+z}} \right) \quad . \quad (67)$$

For the number-redshift relation we get accordingly

$$\log_{10} N_{literature}(z; N_0) = 3 \log_{10} \left(1 - \frac{1}{\sqrt{1+z}} \right) + 3 \log_{10}(1+z) + \log_{10} N_0 \quad . \quad (68)$$

All three equations also result from the well-known Mattig equation (1958), if the delay parameter $q_0 = 1/2$ is set there, whereby this equation describes a flat universe {see e.g. A. R. Sandage et al. [10]}.

We have used Eq. (67) in the measured value diagram Fig. 11 for comparison with the theory presented here.

6. Final considerations

6.1 Hubble parameter

At this point we explicitly point out that our equation of today's Hubble parameter - which also only applies to very small redshifts - differs significantly from the definition (!) used in the specialist literature. The equations for both are

$$H_{0a} \approx \frac{c_0}{\left(\frac{1}{2\beta_{0m}} \frac{1}{\sqrt{\Omega_{0rm} + 1}} + 1 \right) R_{0a}} \quad (we)$$

and

$$H_{0,lit} = \frac{\dot{a}_0}{a_0} = \frac{\dot{a}_0 r_a}{a_0 r_a} = \frac{\dot{R}_{0a}}{R_{0a}} \quad r_a = const \quad (literature) \quad . \quad (69)$$

For an arbitrary point in time t this is

$$H_a(t) \approx \frac{1}{\left[\frac{1}{2\beta_m(t)} \frac{1}{\sqrt{\Omega_{rm}(t) + 1}} + 1 \right]} \frac{c_0}{a(t)r_a} = \frac{1}{\left[\sqrt{\frac{a(t)r_a}{R_s}} \frac{1}{\sqrt{\Omega_{rm}(t) + 1}} + 1 \right]} \frac{c_0}{a(t)r_a} \quad (we)$$

$$\text{because of} \quad \frac{1}{\beta_m(t)} = 2\sqrt{\frac{R_a(t)}{R_s}} = 2\sqrt{\frac{a(t)r_a}{R_s}} \quad \text{being} \quad \frac{c_0}{r_a} = const \quad \frac{r_a}{R_s} = const \quad R_s = const$$

and

(69a)

$$H_{a,lit}(t) = \frac{\dot{a}(t)r_a}{a(t)r_a} \quad (literature) \quad .$$

The index a generally indicates the spatial proximity to the observer, meaning $r = r_a$.

In our theory, the numerator contains the constant physical speed of light c_0 in vacuum, while the current, i.e. the variable spatial expansion speed da/dt is found at this point in the specialist literature.

In the more recent past - time t_x - our distance from the coordinate origin $R_{xa} < R_{0a}$ was slightly smaller than the current one and the Hubble parameter H_{xa} was therefore correspondingly larger (also via the parameter β_{xm}).

In the case of the Hubble parameter in specialist literature, the - actually non-physical - spatial expansion speed da/dt can have been arbitrarily large and, in addition, the scale parameter $a(t)$ arbitrarily small.

Both types of Hubble parameters therefore show a completely different behavior!

In addition, our Hubble parameter is actually made up of physical quantities, while the Hubble parameter in the astrophysical literature is only defined using the non-physical scale parameter $a(t)$, even if the latter can be

assigned a suitable unit of measurement - e.g. Mpc. This means that $a(t)$ alone per se is not a physical distance. This meaning only applies to the real physical distance $R(t) = a(t) r$ and the differences that can be calculated from it.

The Hubble parameter is the proportionality factor between the Hubble speed $V = c_0 z$ and a distance, i.e. the actual Hubble law applies

$$V = c_0 z = H_{0a} D \approx \frac{1}{\left(\frac{1}{2\beta_{0m}} \frac{1}{\sqrt{\Omega_{0rm} + 1}} + 1 \right)} \frac{c_0}{R_{0a}} D \quad (we)$$

and

$$V_{lit} = c_0 z = H_{0,lit} D_{lit} = \frac{\dot{a}_0}{a_0} D_{lit} = \frac{\dot{R}_{0a}}{R_{0a}} D_{lit} \quad (literature) \quad . \quad (70)$$

For the redshift z it simply follows therefore

$$z = \frac{H_{0a}}{c_0} D \approx \frac{1}{\left(\frac{1}{2\beta_{0m}} \frac{1}{\sqrt{\Omega_{0rm} + 1}} + 1 \right)} \frac{D}{R_{0a}} \quad (we)$$

and

$$z = \frac{H_{0,lit}}{c_0} D_{lit} = \frac{\dot{a}_0}{c_0} \frac{D_{lit}}{a_0} = \frac{\dot{R}_{0a}}{c_0} \frac{D_{lit}}{R_{0a}} \quad (literature) \quad . \quad (71)$$

In the literature, the redshift z is therefore depending on the ratio of the current speed of the observer (his galaxy) related to the origin of the coordinates to the speed of light in the product with the ratio of an object distance D_{lit} and the current distance of the observer's galaxy from the origin of the coordinates.

Our redshift, on the other hand, is depending on the ratio of the light path distance D and the current distance R_{0a} of the observer galaxy from the coordinate origin and is besides proportional to the factor that contains the parameter β_{0m} .

Using the parameter β_{0m}

$$\frac{1}{\beta_{0m}} = 2 \sqrt{\frac{R_{0a}}{R_S}} \quad with \quad R_S = \frac{2M_{Fs} G}{c_0^2} \quad (29a)$$

we see in our case

$$z = \frac{H_{0a}}{c_0} D \approx \frac{1}{\left(\sqrt{\frac{R_{0a}}{R_S} \frac{1}{\sqrt{\Omega_{0rm} + 1}} + 1}} \right)} \frac{D}{R_{0a}}, \quad (72)$$

i.e. an direct dependence on the Schwarzschild radius R_S , or more precisely on the ratio R_{0a} to R_S .

Overall, it is somewhat unclear in the specialist literature what exactly corresponds to the distance D_{lit} .

Note:

Of course, it can be set $\Omega_{0rm} = 0$ in equations (70) to (72) in case of neglecting the radiation matter.

Fig. 20 shows the difference between our non-approximated redshift distance D and the linear Hubble redshift distance that is an approximated one.

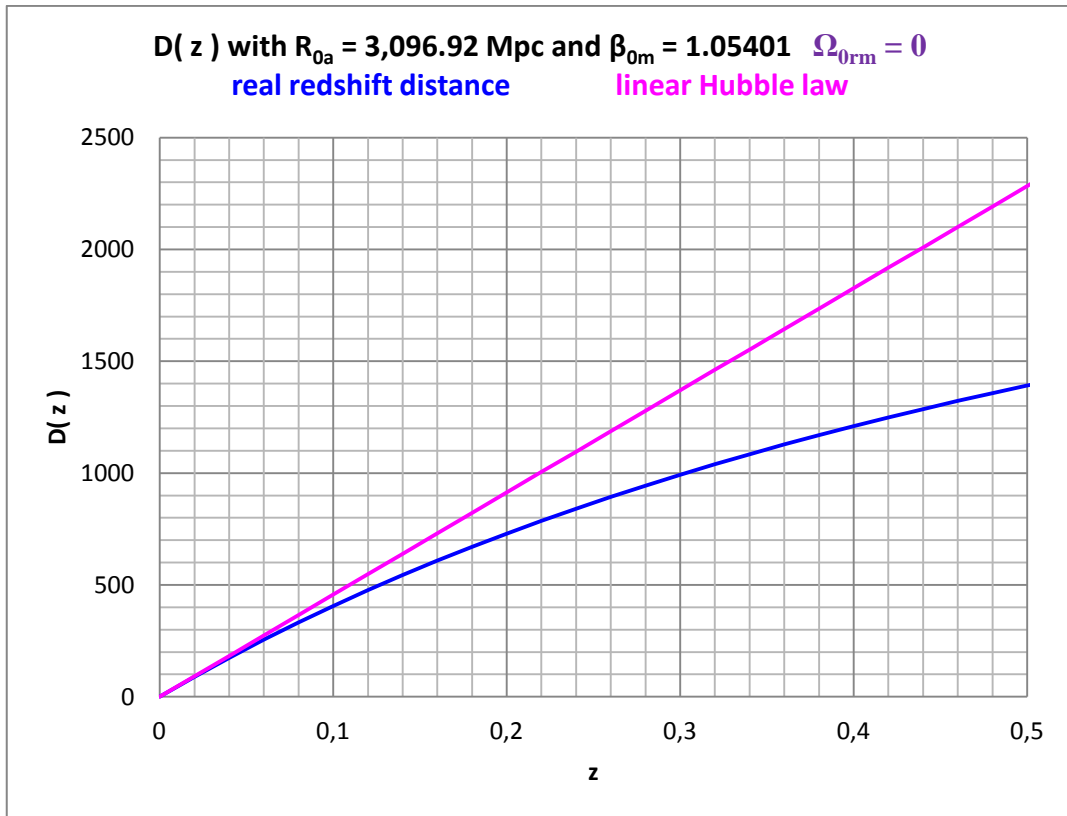


Figure 20. Non-approximated redshift distance D compared to the linear Hubble redshift distance.

It can be seen that the two curves already clearly separate from each other at $z \approx 0.04$, and that Hubble's law results in distances that are significantly too large for larger redshifts, so that it is no longer applicable from around this value.

Recall:

Of course, it should be noted that the Hubble parameter H_{0a} in our theory results from an approximation for small redshifts z .

6.2 Mean values

If we replace in Eq. (39)

$$m(z; m_{0a}, \beta_{0m}, \Omega_{0mr}) = 5 \log_{10} \left\{ \frac{1}{\beta_{0m}} \left[\sqrt{1 + \Omega_{0mr}} - \sqrt{\Omega_{0mr} + \frac{1}{(1+z)}} \right] + z \right\} - 5 \log_{10}(1+z) + m_{0a} \quad (39)$$

the parameter m_{0a} using the equation (with the absolute magnitude M)

$$m_{0a} = 5 \log_{10}(R_{0a}) - 5 + M \quad [R_{0a}] = pc \quad (60a)$$

we get

$$m(z; m_{0a}, \beta_{0m}, \Omega_{0mr}) = 5 \log_{10} \left\{ \frac{1}{\beta_{0m}} \left[\sqrt{1 + \Omega_{0mr}} - \sqrt{\Omega_{0mr} + \frac{1}{(1+z)}} \right] + z \right\} - 5 \log_{10}(1+z) + 5 \log_{10}(R_{0a}) - 5 + M \quad (73)$$

From this equation it follows immediately

$$R_{0a}(z; m, M, \beta_{0m}, \Omega_{0mr}) = \frac{(1+z)}{\left\{ \frac{1}{\beta_{0m}} \left[\sqrt{1 + \Omega_{0mr}} - \sqrt{\Omega_{0mr} + \frac{1}{(1+z)}} \right] + z \right\}} 10^{\frac{(m-M)}{5} + 1} \quad (74)$$

or, if we introduce the distance module $\mu = m - M$

$$R_{0a}(z; \mu, \beta_{0m}, \Omega_{0mr}) = \frac{(1+z)}{\left\{ \frac{1}{\beta_{0m}} \left[\sqrt{1 + \Omega_{0mr}} - \sqrt{\Omega_{0mr} + \frac{1}{(1+z)}} \right] + z \right\}} 10^{\frac{\mu}{5} + 1} \quad \text{with} \quad \mu = (m - M) \quad (74a)$$

Note:

While the redshift z and the apparent magnitude m are actual measured variables, the distance module μ has to be regarded as a parameter because the absolute magnitude M cannot be measured directly.

The parameter β_{0m} is known to us from the evaluation of the Quasar catalog by Véron-Cetty [1]. In [3] the following parameters characterizing all 27 SN Ia are given: absolute magnitude M_B , redshift z and maximum apparent magnitude m_B .

This allows us to calculate the associated $R_{0a,i}$ for all SN Ia_{*i*} (*i* numbers the individual SN Ia). Table 6 shows the result:

z_i	$R_{0a,i}$ [Mpc]	z_i	$R_{0a,i}$ [Mpc]	z_i	$R_{0a,i}$ [Mpc]
0.004356347	3,066.2772	0.002298257	3,413.7353	1.008452514	2,465.7043
0.003502423	2,991.6232	0.003492416	3,573.9143	1.004563157	3,210.5500
0.004356347	3,066.2772	0.006217635	3,492.2585	1.001517717	2,971.7875
0.002298257	3,275.1398	0.008078922	3,253.6726	1.004356347	3,010.3113
0.003502423	4,120.0918	0.007485178	2,559.8100	1.003502423	3,139.8355
0.003502423	3,082.5270	0.004356347	3,066.2772	1.004343005	2,903.5977
0.005176915	3,581.8134	0.006614576	2,373.7888	1.004826672	3,375.5019
0.006291019	3,221.4388	0.004356347	3,010.3113	1.004703254	2,841.3293
0.004563157	3,504.1238	0.005677261	2,383.9837	1.0042396	3,313.9533
< R_{0a} > =	3,121.0976				

Table 6. Various distances $R_{0a,i}$ of the 27 SN Ia_{*i*} calculated using the distance modules μ_i .

It may seem strange that we get a different value for $R_{0a,i}$ for each SN Ia_{*i*}, which is actually the current physical distance of the observer from the coordinate origin with $r = 0$. In particular, the $R_{0a,i}$ for almost equal redshifts z_i should match!

Nevertheless, if we form the mean value of the 27 calculated values $R_{0a,i}$, we find $\langle R_{0a} \rangle \approx 3,121.10$ Mpc. This value is very close to the value $R_{0a} \approx 3,096.92$ Mpc, which we have found analyzing the data.

Overall, we must obvious conclude that the part of cosmology we are considering is essentially a science of averages.

In principle, this could be seen clearly already from the beginning, if we retrospectively look a little more closely about the evaluation of data we carried out, e.g. the quasar catalog and the subsequent finding of R_{0a} .

Only the consideration of a large number of cosmic objects results in the correct values of astrophysical and cosmological relevant quantities, respectively, which then are partly mean values only.

7. Concluding remarks

The real light path $D(z)$ of the photons through the expanding universe corresponds to a dynamic distance and appear therefore as an apparent one. This distance is not identical to the today's distance $D_0(z)$ between the cosmic objects.

For every conceivable observer, the cosmic objects are not spatially, where they appear at first glance!
 In cosmology, nothing is what it seems to be if we look at distances and therefore in the past.

Of course, all cosmological relevant astrophysical objects have a today's distance $D_0(z)$. However, this is not observable, but we can calculate it. Photons that are emitted at this distance from the observed galaxy cannot have reached us so far.

A fundamental property of quantum mechanics is that it can only make probability statements about the microscopic objects it deals with. Here it is seen that both the measuring and the theorizing astrophysics and cosmology, respectively, strictly speaking, can only make statements about mean values of very distant and large numbers of cosmic objects.

This may be one of the reasons why both theories - the theory for the extremely small and the theory for the extremely large - do not fit together, i.e. cannot be brought together.

Note of thanks:

I would like to thank my wife for the long-standing toleration and the corresponding endurance of my almost constant virtual absence. What would I be without her?!

8. Appendix

In this table appendix, we provide the essential data that we have used and some of the data that we have edited or generated for general purposes.

$\langle V \rangle_i$	$\langle z \rangle_i$	$\langle V \rangle_i$	$\langle z \rangle_i$	$\langle V \rangle_i$	$\langle z \rangle_i$
17.12072194	0.269543711	19.5118161	1.28508799	19.7439932	1.86740102
18.42994924	0.434725324	19.4960406	1.30997857	19.7431839	1.90379949
18.77986464	0.514410603	19.5406994	1.33635871	19.73815	1.91629442
18.92177101	0.571495206	19.5648675	1.36044896	19.7370051	1.94113536
19.01993232	0.621120135	19.5526283	1.38646193	19.6390299	1.96661139
19.07454597	0.665043993	19.5667343	1.41249746	19.7247377	1.99498872
19.10685279	0.710045685	19.5917766	1.43823632	19.7073435	2.02761873
19.20756345	0.750830795	19.5835759	1.46348111	19.7225437	2.05895826
19.23878173	0.788362662	19.6146701	1.4877084	19.7209927	2.09067964
19.34673999	0.823077834	19.6560914	1.50872984	19.7166723	2.12286464
19.35605189	0.857111675	19.6421545	1.53039989	19.7562211	2.15726452
19.35379019	0.889902425	19.6730062	1.55031021	19.6955838	2.1915251
19.35354202	0.925268472	19.669718	1.57141117	19.7102256	2.23148844

19.36111675	0.958962211	19.691489	1.59370615	19.6203328	2.27565595
19.36687535	0.99085674	19.6689622	1.61663057	19.6516638	2.32895262
19.39208122	1.021072758	19.7130344	1.64024196	19.7034969	2.39616356
19.41216018	1.049862944	19.7208742	1.66227637	19.6915454	2.47184715
19.43737733	1.076128596	19.7568415	1.68460462	19.7660462	2.57089058
19.47736041	1.10186802	19.6973942	1.70912747	19.7708009	2.71401918
19.4307727	1.129618161	19.7453187	1.7323057	19.7781162	2.90122279
19.45345178	1.157690919	19.7723632	1.75403384	19.9208291	3.05796277
19.4499718	1.18469656	19.7568754	1.77625888	20.0279357	3.20401523
19.50609701	1.208890017	19.7599436	1.79742358	20.2283362	3.40521263
19.48940778	1.233098139	19.7587704	1.82113988	20.5549521	3.7254264
19.47597857	1.259028765	19.7435195	1.84394303	21.3169261	4.34427862

Table 7. Mean values from the quasar data set used according to [1].

Hint:

$\langle z \rangle_i$ (with $i = 1, 2, \dots, 75$) are the 75 mean values of the redshifts of the quasars in the redshift intervals formed.

$\langle V \rangle_i$ are the associated 75 mean values of the apparent visual magnitude of the quasars.

z_i (end of interval)	N_i	z_i (end of interval)	N_i
0.24669	622	3.45369	128,884
0.49338	3,891	3.70038	130,205
0.74008	12,827	3.94708	131,357
0.98677	25,495	4.19377	132,019
1.23346	41,724	4.44046	132,432
1.48015	58,818	4.68715	132,669
1.72685	78,456	4.93385	132,848
1.97354	97,109	5.18054	132,902
2.22023	110,358	5.42723	132,924
2.46692	117,810	5.67392	132,932
2.71362	121,463	5.92062	132,949
2.96031	123,820	6.16731	132,972
3.20700	126,835	6.41400	132,977

Table 8. Numbers N_i summed up in the redshift intervals z_i of the quasars according to [1].

SN Ia	μ_{TRGB}	μ_{Ceph}	μ or $\langle \mu \rangle$	m_{CSP_B0}	m_{SC_B}	m_B or $\langle m_B \rangle$	M_i or $\langle M_i \rangle$	V_{NED}	z
1980N	31.46		31.46	12.08		12.08	-19.38	1,306.00	0.004356347

1981B	30.96	30.91	30.94	11.64	11.62	11.63	-19.31	1,050.00	0.003502423
1981D	31.46		31.46	11.99		11.99	-19.47	1,306.00	0.004356347
1989B	30.22		30.22	11.16		11.16	-19.06	689.00	0.002298257
1990N		31.53	31.53	12.62	12.42	12.52	-19.01	1,050.00	0.003502423
1994D	31.00		31.00	11.76		11.76	-19.24	1,050.00	0.003502423
1994ae	32.27	32.07	32.17	12.94	12.92	12.93	-19.24	1,552.00	0.005176915
1995al	32.22	32.50	32.36	13.02	12.97	13.00	-19.37	1,886.00	0.006291019
1998aq		31.74	31.74	12.46	12.24	12.35	-19.39	1,368.00	0.004563157
1998bu	30.31		30.31	11.01		11.01	-19.30	689.00	0.002298257
2001el	31.32	31.31	31.32	12.30	12.20	12.25	-19.07	1,047.00	0.003492416
2002fk	32.50	32.52	32.51	13.33	13.20	13.27	-19.25	1,864.00	0.006217635
2003du		32.92	32.92	13.47	13.47	13.47	-19.45	2,422.00	0.008078922
2005cf		32.26	32.26	12.96	13.01	12.99	-19.28	2,244.00	0.007485178
2006dd	31.46		31.46	12.38		12.38	-19.08	1,306.00	0.004356347
2007af	31.82	31.79	31.81	12.72	12.70	12.71	-19.10	1,983.00	0.006614576
2007on	31.42		31.42	12.39		12.39	-19.03	1,306.00	0.004356347
2007sr	31.68	31.29	31.49	12.30	12.24	12.27	-19.22	1,702.00	0.005677261
2009ig		32.50	32.50	13.29	13.46	13.38	-19.13	2,534.00	0.008452514
2011by		31.59	31.59	12.63	12.49	12.56	-19.03	1,368.00	0.004563157
2011fe	29.08	29.14	29.11	9.82	9.75	9.79	-19.33	455.00	0.001517717
2011iv	31.42		31.42	12.03		12.03	-19.39	1,306.00	0.004356347
2012cg	31.00	31.08	31.04	11.72	11.55	11.64	-19.41	1,050.00	0.003502423
2012fr	31.36	31.31	31.34	12.09	11.92	12.01	-19.33	1,302.00	0.004343005
2012ht		31.91	31.91	12.66	12.70	12.68	-19.23	1,447.00	0.004826672
2013dy		31.50	31.50	12.23	12.31	12.27	-19.23	1,410.00	0.004703254
2015F		31.51	31.51	12.40	12.28	12.34	-19.17	1,271.00	0.0042396
						<M>=	-19.24		

Table 9. Summary of the data which we have used from the 27 SN Ia according to [3].

SN Ia values that can be traced back to a mean value are marked in **green** (bold).

The individual meanings of the data can be found in the article mentioned.

The data for the angular-size redshift diagram can be found in full in [2].

References

- [1] M.-P. Véron-Cetty and P. Véron, A Catalogue of Quasars and Active Nuclei, 13th edition, March 2010, http://www.obs-hp.fr/catalogues/veron2_13/veron2_13.html
- [2] K. Nilsson, M. J. Valtonen, J. Kotilainen and T. Jaakkola, *Astro. J.* 413 (1993), 453.
- [3] W. L. Freedman u. a., The Carnegie-Chicago Hubble Program. VIII. An Independent Determination of the Hubble Constant Based on the Tip of the Red Giant Branch, arXiv.org:1907.05922
- [4] The Planck Collaboration: Planck 2018 results. VI. Cosmological parameters, arXiv:1807.06209
- [5] The Event Horizon Telescope Collaboration, *The Astrophysical Journal Letters*, 875:L1 (17pp), 2019 April 10, <https://doi.org/10.3847/2041-8213/ab0ec7>
- [6] de.wikipedia.org/wiki/Messier_87, retrieved 18.12.2021
- [7] de.wikipedia.org/wiki/Quasar, retrieved 18.12.2021
- [8] de.wikipedia.org/wiki/UDFj-39546284, retrieved 18.12.2021
- [9] G. Dautcourt, *Was sind Quasare?*, S. 68, Abb. 18, BSB B.G. Teubner Verlagsgesellschaft, 4. Auflage 1987
- [10] A. Sandage, R. G. Kron, and M. S. Longair, *The Deep Universe*, Springer-Verlag, 1995, (Saas-Fee Advanced Course 23, Lecture Notes 1993, Swiss Society for Astrophysics and Astronomy, Publishers: B. Binggeli and R. Buser).
- [11] St. Haase, New derivation of redshift distance without using power expansions, *Fundamental Journal of Modern Physics*, Volume 17, Issue 1, 2022, Pages 1-40
This paper is available online at <http://www.frdint.com/>
-

Copyright:

This text is subject to German and international copyright law, i.e. the publication, translation, transfer to other media, etc. - including parts - is permitted only with the prior permission of the author.

Copyright by Steffen Haase, Germany, Leipzig (2005, 2020, 2022, 2023)